Engineering Structures

# Distributed Sensing (DOFS) in Reinforced Concrete members for reinforcement strain monitoring, crack detection and bond-slip calculation.

--Manuscript Draft--

| | |
|---|---|
| **Manuscript Number:** | ENGSTRUCT_2020_796R1 |
| **Article Type:** | Research Paper |
| **Keywords:** | DOFS; Reinforced Concrete; Distributed sensing; reinforcement strain; bond-slip. |
| **Corresponding Author:** | Mattia Francesco Bado<br><br>Vilnius, Lithuania |
| **First Author:** | Mattia Francesco Bado |
| **Order of Authors:** | Mattia Francesco Bado |
| | Gintaris Kaklauskas |
| | Joan R. Casas |
| **Manuscript Region of Origin:** | Europe |
| **Abstract:** | Distributed Optical Fiber Sensors (DOFS) are novel and increasingly popular strain monitoring tools recently applied to the Structural Health Monitoring (SHM) of Reinforced Concrete (RC) structures. Up to now, most applications have seen the instrumenting of the latter's external surfaces yet, in few circumstances, this technique has also been adopted with the scope of measuring the strains present on the embedded reinforcement bars (rebars). Before the advent of DOFS, due to the lack of tools able to perform such investigation in an accurate, completely-distributed and un-intrusive fashion, structural analyses that rely on the knowledge of the rebars' strains (such as tension stiffening) have always resorted to theoretical, empirical or numerical solutions. Yet, with the potential provided by DOFS, such insight is finally acquirable and represents the start of a new way of understanding the composite behavior of RC structures. The experimental campaign, topic of the present article, intends on taking full advantage of such potential to study the bond stress and slip present on the surface between concrete and steel rebars in differently sized cracking and non-cracking RC tensile members. These are key parameters for the development of any stress transfer approach-based RC structures' serviceability analysis, thus the importance of using DOFS for this novel application. The DOFS extracted bond/slip laws are further compared with the Model Code 2010's predictions and seems to provide consistently higher bond stresses per similar slip than the latter. |
| **Suggested Reviewers:** | Carlos Gil Berrocal<br>carlos.gil@chalmers.se<br>Expertise on Distributed Sensing |
| | Lluis Torres<br>lluis.torres@udg.edu<br>Expertise on steel/concrete bond stress and serviceability analysis |
| | Xavier Chapeleau<br>xavier.chapeleau@ifsttar.fr<br>Experience with Distributed Sensing |
| **Opposed Reviewers:** | |
| **Response to Reviewers:** | |

Dear Editor,

We are pleased to submit an original research article entitled “Distributed Sensing (DOFS) in Reinforced Concrete members for reinforcement strain monitoring, crack detection and bond-slip calculation” by Mattia Francesco Bado (corresponding author), Joan Ramon Casas and Gintaris Kaklauskas for consideration for publication in Engineering Structures. The manuscript is submitted exclusively to Engineering Structures. All authors have approved the submission of the manuscript.

In this manuscript, we study the performance of the cutting edge Structural Health Monitoring tool Distributed Optical Fiber Sensors when bonded to a reinforcement bar later embedded in a Reinforced Concrete (RC) element. In particular, we analyze its ability to measure strains, detect cracks and study the bond-slip phenomenon occurring on the concrete/steel contact surface. The outcome of this research is tightly linked to the study of concrete based composite structures phenomena such as tension stiffening, cracking and more.

We strongly believe that this manuscript is appropriate for publication by Engineering Structures because it brings new insights into a state of the art method of monitoring the inner-workings of RC structures thanks to a novel application.

Thank you for your consideration.

Sincerely,

Mattia Francesco Bado

Department of Reinforced Concrete Structures and Geotechnics, Vilnius Gediminas Technical University/VGTU, Sauletekio 11, Vilnius 10223, Lithuania
E-mail address: mattia-francesco.bado@vgtu.lt

Department of Civil and Environmental Engineering, Universitat Politècnica de Catalunya (UPC), Campus Nord, Carrer de Jordi Girona, 1, 3, 08034 Barcelona, Spain
E-mail address: mattia.francesco.bado1@upc.edu

**Editor and Reviewer Comments:**

*We thank the reviewers for their suggested improvements and corrections. Hopefully the new reviewed version of the paper answers to all the raised points, suggestions and corrections.*

**Reviewer 1**

Your paper presents an interesting experimental campaign. However, there are some issues I would like to see addressed before I can recommend acceptance of your paper as listed below.

*The authors thank the reviewer for the positive comment and the consistently accurate improvement suggestions*

1. Grammar: there are quite a few grammatical mistakes and really odd (and incorrect) words choices. I have tried to highlight the ones that actually make it difficult to understand the paper but once all the other comments are addressed, the paper should be thoroughly proof read by a fluent English speaker.

*This issue was raised by all the reviewers of the present article; thus the authors have decided to submit it to a thorough proofing process from a mother tongue English speaker's part consisting of revision, correction, reformulations and more. Hopefully the article's readability is much improved since the previous version. Furthermore, it should be mentioned that the figures too have received a certain overhaul. Indeed, their spaces have been optimized, their resolution increased (turned to vectorial wherever possible for zero resolution losses) and integrated wherever it was requested by the reviewers.*

2. Please add line numbers to future versions of this paper to make it easier to review.

*The correction was performed.*

3. Abstract: the use of the expression "excellent tools" is poor technical writing as excellent is a highly subjective word. Plus it makes your work sound more like a sales brochure than a technical paper. Please focus on why you think they are excellent.

*The authors agree with such observation and the adjective was removed and substituted by Line 1: "novel and increasingly popular strain monitoring tools".*

4. Abstract: you state "Yet, in hardly any circumstance this technique has been adopted with the scope of measuring the strains present on a reinforcement bar (rebar) embedded inside a RC tensile member (RC tie)." but as you will see in my comments on your literature review, this is not exactly true. Please soften this comment to reflect the existing work.

*The authors agree with such observation and have decided to formulate the sentence as follows Line 11: "in few circumstance this technique". This should answer the raised issue.*

5. Abstract: you state "An accurate, completely-distributed, experimentally measured strain profile of a rebar embedded in a RC structure under different loading conditions, both before and after concrete cracking has been, up until now, impossible.". This statement is misleading as such profiles exist in the published literature. This statement also requires modification.

*The authors agree with such observation and have reformulated the sentence into Lines 13-15: "Before the advent of DOFS, due to the lack of tools able to perform such investigation in an accurate, completely-*

*distributed and un-intrusive fashion, structural analyses that rely on the knowledge of the rebars' strains (such as tension stiffening) have always resorted to theoretical, empirical or numerical solutions."*

6. Pg 4: in the statement "A methodology of studying such relationship exploits the measurement of strains suffered by the reinforcement bars embedded into the concrete." Please change "the measurement of strains suffered by the reinforcement" to "the measurement of strains along the reinforcement". This comment applies throughout the paper when referring to rebar strain since rebars cannot "suffer", only living things can suffer.

*The authors agree with such observation and have removed this term in all the article when referred to the rebars' strains.*

7. Pg 4: you state "DOFS (Figure 1) are very thin glass wires (125 μm of diameter, similar to a hair's thickness)" but this dimension varies based on fiber selection. Please indicate this in the text.

*The protective coating is what increases numerous fold the fiber's diameter but an uncoated fiber has the here mentioned diameter. As such was not mentioned in the article, the authors have made the following corrections. Lines 78-79: "Simple DOFS, without any coating layers (**Error! Reference source not found.**), are very thin glass wires (125μm of diameter, similar to a hair's thickness)...".*

8. Pg 5: the referencing in this statement "in (Sieńko et al. 2018)23 where" is not correct. Delete the brackets and the date.

*The brackets have been removed.*

9. Pg 5: you state "The combination of the two fibers was again used by the same authors in an attempt to measure the shrinkage and tension stiffening of RC ties" but looking at the reference list it does not appear to be the same authors.

*The sentence was streamlined as follows Lines 90-92: "Previous DOFS monitored RC tie tests are reported in Davis et al.[20,21] where the fibers are glued to the degreased reinforcement bars along their longitudinal rib with the intention of monitoring the impact of corrosion and shrinkage on the performance of the members and on its tension stiffening phenomenon.". Furthermore, the two references have now been revised.*

10. Pg 5: The authors appear to be missing key literature from the ACI structural journal. Two papers from Hoult's group seem to me to be using the exact same approach (i.e. the combination DFOS and DIC). The authors need to include these papers and discuss how the current work differs from what is already published. Also, the fact that this work is published makes some of the comments in the abstract slightly misleading in my opinion. See:

Brault, A., & Hoult, N. A. (2019). Distributed Reinforcement Strains: Measurement and Application. ACI Structural Journal, 116(4).

and

Poldon, J. J., Hoult, N. A., & Bentz, E. C. (2019). Distributed Sensing in Large Reinforced Concrete Shear Test. ACI Structural Journal, 116(5), 235-245.

Additionally, this paper recently published in this journal would seem to, based on the title at least, need to be included and discussed:

Broth, Z., & Hoult, N. A. (2020). Dynamic distributed strain sensing to assess reinforced concrete behaviour. Engineering Structures, 204, 110036.

*In order to tackle the raised issues the authors have inserted the following paragraph Lines 111-115: ‘‘Several DOFS-instrumented RC beams tests[24–26] combine the use of fibers and DIC with the intention of relating reinforcement strains with corresponding crack widths, of monitoring the distributed shear strains (shear failures in particular) and of assessing the increase in deflections due to cyclic loading. Despite sharing the same technique (monitoring the members’ superficial strains in order to correlate them to DOFS strain profiles), the DIC is used in the present work as a profile validation and troubleshooting tool rather than as an integral part of the study.” Furthermore, the authors believe the references are also relevant to the present paper as they too deal with DOFS-instrumented rebars embedded inside RC structures with a particular silicone based protection, thus they have referenced it for this too.*

11. Pg 6: you note "reduced cost" as a requirement for sensors. I agree! But how does that happen when DFOS analysers cost $150k? Some discussion of this might be helpful.

*Nowadays the cost of older OBR models mounts up to 40000euros making it a relatively smaller investment. It’s true that the spatial resolution for clear and neat strain profile oscillate around 5mm versus the modern-day interrogator’s 1.3mm (ODiSI-6000) but then again a measurement every 5mm can still yield very accurate profiles too. Once this first investment is made, procuring the DOFS is a very cheap affair. The already calibrated one cost between 50 and 100euros whilst the non-calibrated can cost a third of such price. The authors believe this discussion is out of the scope of the paper especially considering the ever changing panorama of the research tools pricings. The requirement list has now been changed to “performance requirement” list therefore allowing for the removal of “low cost” from it.*

12. Pg 6: I really don't understand what the authors mean in the following statement: "The tensile value applied on the edges of the RC ties is uniformly transmitted all along the rebar, hence equal in every concrete prism located on the same rebar." Please revise.

*The sentence was expanded and reformulated as follows Lines 170-174: “As visible, some RC ties are composed of just one concrete prism (for instance 9x9_D12) whilst others of two (for example member 8x8_D8). On the latter category, being the stresses in a rebar tested in tension uniform along all of its length, the presence of a concrete prism does not influence the steel strains sampled inside another prism positioned along the same bar. Thus, through the casting of two concrete prisms (henceforth referred to as RC block) on a single bar, it is possible to combine multiple RC tie tests in a one.”*

13. Figure ?: Between Tables I and II you have a figure but it is not labeled as such. I think you are trying to call it a part of Table I but it is not at all typical to try to embed figures within tables and it would be better just to make it a stand along figure.

*The authors welcome the reviewer’s suggestion and have accordingly modified the paper.*

14. Pg 8: you state "The members were developed with two concrete baths producing concrete with averaged mechanical properties (compression strength *fc*, tensile strength *fct*, modulus of elasticity *Ec*)" Please describe how these properties (especially fct and Ec) were obtained.

*The following paragraph details the tests used to establish the concrete’s mechanical characteristics Lines 184-195: “The concrete mix used to produce the members consisted of 182 kg/m3 of water, 363 kg/m3 of Portland cement, 968 kg/m3 of fine aggregate and 968 kg/m3 of coarse aggregate (maximum diameter of 12 mm) with an addition of super-plasticizer. The members were developed with three concrete baths producing*

*concrete with averaged mechanical properties established at 28 days in accordance with BS EN 12390 and listed in Table I. The concrete compressive strength fcm was tested on three 150mm cubes, the modulus of elasticity Ecm was tested on three cylinders of size 150mm diameter-300mm height and the tensile strength fctm was established by means of a tensile splitting strength test on three similarly sized cylinders. Additionally, Table I reports the steel yielding strength fy and modulus of elasticity Es established in accordance with ISO 6892-1:2009 (specified in the standard BS EN 10025). ".*

15. Pg 8: you state "at a constant loading speed of 0.1mm/min" however what you give is a displacement rate rather than a loading rate. Please correct the text as necessary.

*The sentence has been rephrased as follows. Lines 197-199: "The members were tested in tension by means of a Universal Testing Machine (UTM). The loading program was a simple displacement-controlled monotonic tensile load increased at a constant speed of 1.0mm/min until the yielding of the rebar is reached."*

16. Pg 8: crucial to the DIC analysis is the pixel to mm conversion factor. The more pixels per mm the more accurate the measurements. Please include that value in the text.

*The authors are in agreement with such observation and therefore introduced in the paper the following sentence Lines 206-208: "In order to act on the first point, the utilized camera was a Canon EOS 77D able to take pictures with a resolution of 6000x4000 pixels (24 megapixels) therefore leading to a ratio between 6.6px/mm and 10px/mm according to the orientation of the shots."*

17. Pg 8: you state "black mate paint" was used but do you mean "black matte paint"?

*The correction has been performed*

18. Figure 5b: I think this data is taken at a specific load step but this is not made clear in the caption or the text. Please specify.

*The authors agree with such correction and Figure 5b has been suitably corrected.*

19. Pg 10 and elsewhere: when you say "polynom", do you mean polynomial? Please correct as needed throughout the paper.

*The authors agree with such correction and have edited it in throughout the whole paper.*

20. Pg 10: you mention a threshold of (100/200 microstrain) as your acceptance threshold. Why did you use this? It seems entirely random. Discuss in the text.

*A deeper explanation has been inserted in an attempt to clarify the sentence Lines 267-269: ". For example, the current test used a 150με threshold as it allowed for the removal of the anomalistic peaks whilst leaving untouched any profile jump resulting from real-life occurrences to the tested member (such as concrete cracking)."*

21. Please replace "naked" throughout the text with the more appropriate "bare".

*The correction has been performed.*

22. Figure 8: it is really not clear what we are looking at here. Can you include an inset figure of the specimen showing what part of it these strains are being measured on?

*The authors agree with such observation and have integrated in the figure an illustration of the members.*

23. Pg 14: you state "Despite good agreement between theoretical and experimental strain profiles is embodied by the strain profiles with behavior A", where do we see this agreement? Figure 8 appeared to only be presenting experimental data so I'm confused by where I should be looking for this agreement?

*The authors agree that the sentence can lead to confusion. Furthermore, the point it originally attempted to make was redundant in nature; therefore, this particular sentence was removed and only the edited version of the following one is kept Lines 385-387: "In order to assess the correctness of these novel assumptions, further studies should be dedicated to the influence of the tested RC members' longitudinal dimensions on the steel strain profiles."*

24. Pg 16: once again I'm afraid the following sentence doesn't really make sense and needs to be rewritten: "It is immediately evident how a variation of the degree of the polynomial approximation alters the shape of the bond-stress diagram as higher degree ones present a higher sensibility to the pendency fluctuations of a strain profile."

*The authors have modified the sentence as follows. Lines 420-424: "Furthermore, in order to clearly see the profile differences arising when using a specific polynomial degree approximation versus all the others, Figure 10 reports all the curves as calculated by means of 4th, 6th and 8th degree polynomial approximations. Their dissimilarity is immediately evident as the ones resulting from higher degree polynomial approximations present more fluctuations as a testament to their increased sensitivity to the strain profiles' own pendence variations.".*

25. Pg 16: you state "The advantages of such sensibility can be seen", I have a feeling you mean "sensitivity" but sensibility is definitely not the right word.

*The authors agree with such observation and have substituted the word "sensibility" with "sensitivity" in all the article.*

26. You seem to spell the word behavior with and without a u in this paper. Please be consistent.

*The authors have rectified this inconsistency.*

27. Pg 19: you state "whose ascending branch's pendency coincides", but I really don't think pendency is an appropriate word choice. Please revise.

*The authors agree with such observation and have substituted the word "pendendcy" with "pendence" in all the article.*

28. Reference 37: Are you sure this is correct? Those last names seem like first names, especially "Sara".

*The authors agree with such observation and have corrected the mentioned reference.*

**Reviewer 2**

The paper presents an interesting topic of the experimental bond tests carried out on RC members using the distributed the optical fiber sensors for strain monitoring, crack detection and bond-slip modelling. DOFS strain profiles were used for crack detection and providing the bond-slip laws.

*The authors thank the reviewer for the positive comment and the consistently accurate improvement suggestions.*

In fact, there are a lot of confusing paragraphs that need corrections and several clarifications. The Authors are requested to make amendments and detailed clarifications according to the following comments:

1. The main doubt of reviewer is lack of clear rules and principles, which were the basis of the test assumptions. Especially that the tested members varies with more than one parameter. As the test program seems to be very random, it rises difficulties in the test analysis. The test program assumptions should be explained to justify the goal of the tests.

   *The authors acknowledge the lack of transparency in the test's goals and assumptions and have accordingly modified Chapter 2.1: Test concept and goals.*

2. It is not clear how the tensile stress was performed. The precise explanation of the load performance would be valuable.

   *The test program has been reformulated and slightly expanded in an attempt to increase its clarity and goes as follows Lines 197-199: "The members were tested in tension by means of a Universal Testing Machine (UTM). The loading program was a simple displacement-controlled monotonic tensile load increased at a constant speed of 1.0mm/min until the yielding of the rebar is reached."*

3. Table I presents 5 types of RC tensile members dimensional and bonding technique representation, however the cross sections presented below the specimens do not correspond to the specific members e.g. cross section for member 10x10_D12 is 9x9 (it should be 9x9_D12) the same with others

   *Table I's errors, converted to Figure 2 as per other reviewer's suggestion, has been corrected and the specimens' geometry is now consistent along all the article.*

4. Table I does not correspond with Table II.

   *Table I's errors, converted to Figure 2 as per other reviewer's suggestion, has been corrected and the specimens' geometry is now consistent along all the article.*

5. There is a confusing sentence: "*Member **9x9_D12's areas hatched in red** correspond to segments where the concrete/rebar bond was ineffective, practically leaving the two materials separated and thus the rebar deprived of any tension stiffening"* in accordance to Table I (the hatched in red part is presented in the member 10x10_D12 not in 9x9_D12, unless the second member should not be 10x10_D12 but 9x9_D12).

   *Table I's errors, converted to Figure 2 as per other reviewer's suggestion, has been corrected and the specimens' geometry is now consistent along all the article.*

6. The next confusing phrase refers to: "*8x8_D8 is generally the hardest to monitor due to its reduced bar diameter and **reduced spacing for the groove** and **the adhesive**."* It seems that the groove spacing in member 8x8_D8 is rather extended not reduced comparing to other specimens.

*The authors agree with the reviewer that the sentence is badly formulated and hard to understand therefore it has been altered to Lines 146-150: "Regarding the third one, it should be mentioned that, up until the present moment, Ø8 is a rebar diameter whose bond stress has hardly been investigated due to its reduced diameter preventing the allocation of relatively bulky sensors (strain gauges with their large cabling or FBG sensors) neither on its surface, nor in its core. Therefore, DOFS is possibly the best and only way to instrument such rebars."*

7. There is difficult to know why the steel strain measured by DOFS (Fig. 4) is zero along the initial not embedded length of the steel bar, but in the latter not imbedded length of the bar, after the second concrete prism of 330 mm the strain curve is cut, without any measurements. Does it mean that the DOFS was not bended along the latter steel bars outside the concrete prism?

   *The authors have changed Figure 4 in an attempt to clarify the raised issues. In particular, an illustration of the member has been added to ease the reader's comprehension of what DOFS segment corresponds to what section of the RC tie. The first DOFS segment is not bonded to anything, thus labeled with "unbonded DOFS", whilst the second segment is integrally bonded to the rebar, thus labelled "bonded DOFS". In the case of Figure 4, the fiber reads 0με strictly when it is unbonded, therefore only until DOFS coordinate 0.58m (where the "unbonded DOFS" segment finishes and "bonded DOFS" starts). In the second segment, the fact that the DOFS-instrumented rebar is not embedded inside concrete does not mean that its value will be 0με since in those sections the DOFS is measuring the rebar strains.*

8. The specimens 10x10_D12 (a) and 9x9_D12 (b) do not correspond with Table 1, which makes difficulties in proper understanding of the DIC measurement description referring to both members.

   *Table I's errors, converted to Figure 2 as per other reviewer's suggestion, has been corrected and the specimens' geometry is now consistent along all the article.*

9. Figure 8 does not correspond with Table I and Table II.

   *Table I's errors, converted to Figure 2 as per other reviewer's suggestion, has been corrected and the specimens' geometry is now consistent along all the article.*

10. Due to so many mistakes and confused phrases further revision of the test results and bond-slip modelling is not possible. The Authors are requested to perform the major revision of the paper, because it is absolutely not acceptable in this version.

    *The authors recognize the presence of mistakes and grammatically lackluster paragraphs thus the authors have decided to submit the article to a thorough proofing process from a mother tongue English speaker's part consisting of revision, correction, reformulations and more. Hopefully the article's readability is much improved since the previous version. Furthermore, it should be mentioned that the figures too have received a certain an overhaul. Indeed, their spaces have been optimized, their resolution increased (turned to vectorial wherever possible for zero resolution losses) and integrated wherever it was requested by the reviewers.*

Highlights

- Distributed Optical Fiber Sensors as innovative Structural Health Monitoring tools
- Monitoring of reinforcement bars embedded inside Reinforced Concrete structures
- Distributed and real time monitoring of steel strain profiles and crack formation
- Study of steel-concrete bond stress & slip relationship with Distributed Sensing
- DOFS monitored evolution of steel-concrete bond stress & slip during loading

# Distributed Sensing (DOFS) in Reinforced Concrete members for reinforcement strain monitoring, crack detection and bond-slip calculation.

**Mattia Francesco Bado[1,2], Joan R. Casas[1], Gintaris Kaklauskas[2]**

*1. Department of Civil and Environmental Engineering, Technical University of Catalunya. UPC-BarcelonaTech Campus Nord, Calle Jordi Girona 1-3, Barcelona 08034, Spain*

*2. Institute of Building and Bridge Structures, Vilnius Gediminas Technical University, Saulėtekio al. 11, Vilnius 10221, Lithuania*

## Abstract

Distributed Optical Fiber Sensors (DOFS) are novel and increasingly popular strain monitoring tools recently applied to the Structural Health Monitoring (SHM) of Reinforced Concrete (RC) structures. Up to now, most applications have seen the instrumenting of the latter's external surfaces yet, in few circumstances, this technique has also been adopted with the scope of measuring the strains present on the embedded reinforcement bars (rebars). Before the advent of DOFS, due to the lack of tools able to perform such investigation in an accurate, completely-distributed and un-intrusive fashion, structural analyses that rely on the knowledge of the rebars' strains (such as tension stiffening) have always resorted to theoretical, empirical or numerical solutions. Yet, with the potential provided by DOFS, such insight is finally acquirable and represents the start of a new way of understanding the composite behavior of RC structures. The experimental campaign, topic of the present article, intends on taking full advantage of such potential to study the bond stress and slip present on the surface between concrete and steel rebars in differently sized cracking and non-cracking RC tensile members. These are key parameters for the development of any stress transfer approach-based RC structures' serviceability analysis, thus the importance of using DOFS for this novel application. The DOFS extracted bond/slip laws are further compared with the Model Code 2010's predictions and seems to provide consistently higher bond stresses per similar slip than the latter.

## Key words

Distributed Sensing; Structural Health Monitoring; Reinforced concrete; Steel rebar strains; Bond stress

## 1. Introduction

The interaction between concrete and reinforcement bars is the central issue for all RC structures, dictating both their behavior and performance. In general practice, a full interaction between their interfaces with no physical slip is assumed[1], but, whilst this simplification is reasonable in load bearing capacity analysis, it becomes unacceptable when the serviceability of RC structures is considered. For the latter, instead, a *stress transfer approach* (also referred to as partial interaction or discrete crack based approach) is more suitable[2] as it portrays in a more realistic fashion the inner-workings of a RC structure. This approach introduces the idea of a force transfer, defined as *bond stress* $\tau$, occurring along the contact surface of concrete and the embedded steel bars. Furthermore, the bond is suggested to vary according to the concrete/rebar *slip*, representative of their absolute displacements dissimilarity. Indeed, the occurrence of slip usually results in localized concrete damage (especially in proximity to a member's edge or cracked section) which significantly reduces the bond action[3]. Bond stress and slip are the constitutive parameters of the stress transfer approach and thus they cover a crucial role in the serviceability study of RC structures and in providing key elements for a correct development of finite element models on the grounds of which accurate structural evaluations can be developed[4]. Despite such crucial roles and despite having been extensively investigated both analytically and experimentally over the years[5–7], satisfactory bond/slip prediction models have not yet been achieved as testified by the large discrepancies among the existing ones[8,9].

The most recurrent experimental technique for measuring them is the direct pull-out test in which an embedded reinforcement bar is directly pulled out from the concrete interface. Yet, according to modern researchers[1,10], conventional pullout tests fail to provide the real bond conditions because of its support-induced compressive stress field in the concrete, of its non-uniform distribution of bond stresses around the anchorage length and finally due to the instigation of lateral confining pressure at the reinforcement-concrete interface.

Alternatively, a more realistic way to study the bond/slip is the double pullout test. The latter is essentially a tensile RC tie test integrated with monitoring sensors able to sample and report the evolution of the strains along the segment of the reinforcement bars embedded inside concrete. Indeed, RC ties are often used to illustrate cracking, deformation and bond behavior of RC structures thanks to their simplicity and reasonably good representation of the distribution of internal forces and strains in the tensile zone of RC structures[11]. Thus, being the local response of the bond affected in each point by the longitudinal strain state of the bar $\varepsilon_s(x)$, the bond slip behavior is simply obtained by the governing equivalence[3] indicated in Equation 1.

$$\frac{d\varepsilon_s(x)}{dx} = \frac{4}{E_s \emptyset_s}\tau(x) \quad (1)$$

Where $E_s$ represents the steel's modulus of elasticity and $\emptyset_s$ the steel rebar's diameter. Whilst some experimental campaigns[12–14] perform such study on a concrete block defined by two consecutive RC ties' cracks, some others[7,15] do the same on members of length sufficiently reduced not to welcome any transversal cracks during its testing (L < *mean crack spacing value* $s_{rm}$). Effectively, the stress transfer phenomenon occurring on the edges of the former occurs in a similar fashion on the edges of the latter. In both cases the bond action is significantly reduced by the presence of slip-induced localized concrete damage. Therefore, it is safe to assume that the bond-stress present in a cracking RC tie can be simulated by a smaller one with identical cross-sectional dimensions which will additionally be free of cracking-induced uncertainties (such as oblique and/or not fully developed cracks, steel redistribution and double pointed peaks).

In either case, an accurate measurement of the variation of $\varepsilon_s$ along the rebar is the key to an equally accurate bond stress/slip depiction. In the past numerous attempts were developed with the goal of measuring the strains in a RC member's rebar. Kankman[7] instrumented Ø25 bars by first sawing them in two, longitudinally-wise, and later milling their core in order to provide 6 mm wide/5 mm deep and 9.5 mm wide/4 mm deep channels for the installation of 3 mm and 5mm long strain gauges respectively. Houde[12], Beeby and Scott[16] and Scott and Gill[13] proceeded in their tests in a very similar manner. Despite the revolutionary aspect of such test at the time, the technique is time-consuming, labor-intensive, and rather invasive. All of this in addition to being punctual in nature (Kankman positioned the strain gauges at 25mm distance while Houde at 1.5'' corresponding to 38.1mm). A more modern and advanced tool employed for the monitoring of rebars' strains are Fiber Braggs Gratings (FBGs), quasi-distributed optical fiber sensors in which a characteristic wavelength is used to simultaneously provide its address in the sensor network, and the measurement (temperature and strains)[17]. Kaklauskas et al.[1] installed FBG sensors on the surface of a rebar (positioned inside a 2 mm wide/1.5 mm deep groove) before embedding it inside a RC tie. In this case, the spatial resolution was 20mm.

The present paper opts, instead, to study the strain distribution along the rebar with yet a different tool; Distributed Optical Fiber Sensors (DOFS) which, despite sharing with FBGs the same functioning principle (transmission of light pulses through a glass medium), is quite different performance-wise. Simple DOFS, without any coating layers (Figure 1), are very thin glass wires (125μm of diameter, similar to a hair's thickness) able to accurately measure strains (with an accuracy of 1με[18]), temperature and vibration in 2 or even 3 dimension and in a completely distributed manner (even every millimeter) with flexible spatial resolution and desired frequency. The functioning of these sensors is based on the fact that, assuming the characteristics of the light transmission within a fiber well known and the latter properly calibrated, any alteration (due to temperature and strain) are detected through back-scattered light by the Optical Backscatter Reflectometer (OBR) and finally translated to strain variation in each of the DOFS' points[19]. The instrumenting of structural elements with DOFS is simple, rapid and very little invasive as it consists only of covering the fiber with adhesive while the former is correctly positioned on the element to monitor. Seen the large amount of advantages that this tool boasts, its increasing popularity is quite understandable.


(a) (b)

***Figure 1.*** *Distributed Optical Fiber Sensor with loose termination (b) and bonded to a rebar*

Previous DOFS monitored RC tie tests are reported in Davis et al.[20,21] where the fibers are glued to the degreased reinforcement bars along their longitudinal rib with the intention of monitoring the impact of corrosion and shrinkage on the performance of the members and on its tension stiffening phenomenon. Sieńko et al. 2018[22] also report a DOFS monitored RC tie test where the fiber is glued to the degreased reinforcement bar parallelly to the longitudinal rib with an epoxy resin. The fiber under consideration, though, differs from the current test's due to the presence of a protective jacket that consequently increases the diameter of the sensor around 7 folds (0.125mm versus 0.9mm).

Considering the intrinsic sensitive nature of these thin DOFS, a certain amount of protection is required whenever embedding them inside RC structures. In order to do so, some authors[23] designed a method consisting of incising a groove on the side of the rebar (along the longitudinal ridge) and positioning the DOFS inside it (as visible in Figure 1b) finally securing the bond with adhesive. The current experiment embraces this methodology using cyanoacrylate as bonding adhesive. Only one RC sample, takes cue from Hoult et al.[24–26]'s work and includes an extra layer of silicone on top of the bonded DOFS for even further protection.

Finally, the results shown in the present publication are integrated and validated with the external monitoring method of Digital Image Correlation (DIC). The latter is an innovative, cheap non-contact optical technique for measuring strain and displacement. DIC works by comparing digital photographs of a component or test piece at different stages of deformation. By tracking blocks of pixels of a complex stochastic pattern, the system can measure surface displacement and build a 2D and 3D deformation vector fields and strain maps[27]. DIC utilizes a correlation algorithm to obtain displacements and deformations by identifying areas of matching grey-scale values between the stochastic pattern of the deformed and un-deformed images[28]. This analysis was developed with the help of GOM Correlate software by GOM Precise Industrial 3D Metrology.

Several DOFS-instrumented RC beams tests[24–26] combine the use of fibers and DIC with the intention of relating reinforcement strains with corresponding crack widths, of monitoring the distributed shear strains (shear failures in particular) and of assessing the increase in deflections due to cyclic loading. Despite sharing the same technique (monitoring the members' superficial strains in order to correlate them to DOFS strain profiles), the DIC is used in the present work as a profile validation and troubleshooting tool rather than as an integral part of the study.

In conclusion, the experimental campaign, topic of the present article, intends to take full advantage of DOFS' potential to assess the stress transfer approach's main parameters, namely the bond stress and slip, present inside differently sized cracking and non-cracking RC tensile members. This is achieved by means of DOFS' distributed monitoring of their rebars' strains (validated against a simultaneous DIC superficial monitoring) and, through Equation 1, the calculation of their relative bond/slip values. These ones will finally be compared to the values predicted by the Model Code 2010[9]'s.

## 2. The test program

### 2.1 Test concept and goals

The experimental campaign described in the present article is aimed at assessing the stress transfer approach's main parameters, namely the bond stress and slip present between steel and concrete, by means of DOFS-extracted steel strain profiles of rebars embedded inside multiple RC ties. This campaign's experimental effort is intended to represent the beginning of a novel DOFS-aided bond/slip quantification trend which should be as broad and universal as possible in order to encapsulate all the various facets of these phenomena. Consequently, the present campaign not only embraces both above described bond/slip testing methodologies (cracking and non-cracking members) but adds further diversity in its RC samples by varying both their transversal and longitudinal dimensions.

The study of bond stress and slip, despite being key elements for a RC structure's serviceability analysis, has yet to be tackled with modern cutting-edge tools such as DOFS. Consequently, the latter's suitability to provide adequate and accurate results towards such end has yet to be established and represents one of the main goal of this article. Generally speaking, the ideal civil engineering strain monitoring sensors should meet the performance requirements of elevated accuracy, measurement speed, broad sensing field, interference resistance, flexibility, ease of use, resistance, durability, flexible sensing lengths, little intrusiveness, applicability to the broadest range possible of structures, high performance threshold and ease of transportation. In order to achieve the objective of assessing bond/slip inside a RC structure, the previous list's crucial requirements are:

- Measured strains accuracy;
- High spatial resolution in order to increase the number of monitored points;
- Little intrusiveness in order to monitor RC structures without altering their performance and in order to instrument small diameter rebars (Ø8, Ø10);
- Resistance to the friction present between the rebars' surface (where DOFS is bonded) and the concrete whenever slip takes place;
- High strain measuring threshold in order to monitor the rebar's strains until or beyond yielding.

As previously stated the first three points are satisfied by the intrinsic nature of the DOFS itself. Regarding the third one, it should be mentioned that, up until the present moment, Ø8 is a rebar diameter whose bond stress has hardly been investigated due to its reduced diameter preventing the allocation of relatively bulky sensors (strain gauges with their large cabling or FBG sensors) neither on its surface, nor in its core. Therefore, DOFS is possibly the best and only way to instrument such rebars. The last two points are what the positive outcome of the test depends upon. The first of these represents the biggest obstacle and is exacerbated when the concrete enters the cracking phase. Indeed, literature on RC structures experimental campaigns using uncoated DOFS indicates that the appearances of cracks is the singular most disruptive instance of the test as following measurements suffer a great accuracy and reliability loss[20,29–32]. Finally, the last point is directly connected to the former. Indeed, in order for DOFS to meet its requirement, the DOFS/rebar bonding technique should warrant sufficient protection to guarantee that not only the strain measurement accuracy is not affected by the advent of cracks but also that it remains unaltered until/beyond the steel yielding stage. In order to achieve these two requirements, the tested RC ties introduce a longitudinal groove and a protective silicone layer to the DOFS/rebar bonding technology.

### 2.2. Experimental samples description

The samples used in the present experimental campaign are five RC ties with different rebar diameters and concrete prism transversal and longitudinal dimensions. They will henceforth be referred to with a code such 8x8_D8, where the first two numbers are indicative of the cross sectional dimensions (in cm) and the last of the embedded rebar diameter (in mm). For example, member 8x8_D8 refers to a member characterized by a cross-sectional dimension of 80mmx80mm with a Ø8 rebar embedded inside it. Figure 2a introduces the five RC ties together with their geometrical features and DOFS bonding technology.

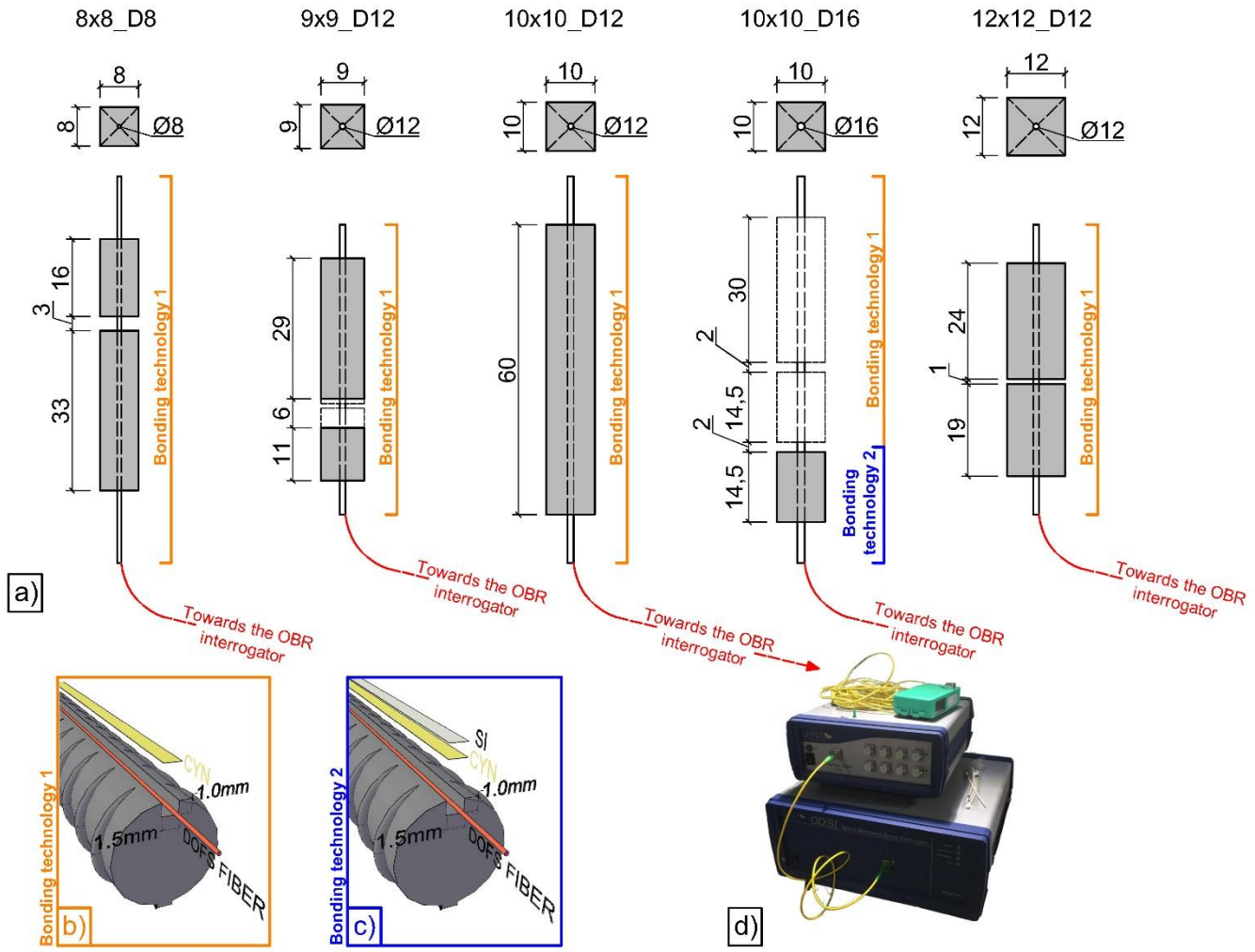


***Figure 2.*** *Tested RC ties' geometrical features (a) with their respective bonding technologies with (c) and without (b) the addition of a protective silicone layer. The DOFS-instrumented rebars were monitored by means of an ODiSI-A OBR interrogator (d).*

As visible, some RC ties are composed of just one concrete prism (for instance 9x9_D12) whilst others of two (for example member 8x8_D8). On the latter category, being the stresses in a rebar tested in tension uniform along all of its length, the presence of a concrete prism does not influence the steel strains sampled inside another prism positioned along the same bar. Thus, through the casting of two concrete prisms (henceforth referred to as RC block) on a single bar, it is possible to combine multiple RC tie tests in a one. For example, member 8x8_D8 (as in Figure 2a) can provide the same results that could be extracted testing separately a 33cm long prism and another 16cm long prism, both having 8x8_D8's cross-sectional features. Member 9x9_D12's unhatched areas correspond to portions of the RC tie where the concrete/rebar connection was absent, practically leaving the two materials separated and the rebar deprived of any tension stiffening effect (as will be visible later on in its strain profile). Concerning the DOFS/rebar bonding technology, every rebar is incised with a groove 1mm deep/1.5mm wide along its longitudinal rib (as in Figure 1) in which the DOFS is later positioned and bonded with cyanoacrylate (CYN) as in Figure 2b or with a combination of CYN and a protective silicone (SI) layer as in Figure 2c. The only member using SI in correspondence to one of its RC blocks is 10x10_D16. For either of the two bonding techniques, before proceeding to the positioning of the DOFS, the contact surface is properly sand-blasted and degreased with alcohol.

The concrete mix used to produce the members consisted of 182 kg/m3 of water, 363 kg/m3 of Portland cement, 968 kg/m3 of fine aggregate and 968 kg/m3 of coarse aggregate (maximum diameter of 12 mm) with an addition

of super-plasticizer. The members were developed with three concrete baths producing concrete with averaged mechanical properties established at 28 days in accordance with BS EN 12390 and listed in Table I.

*Table I. Mechanical properties of the RC tensile member's constitutive materials*

| Members | Concrete | | | Steel | |
|---|---|---|---|---|---|
| | $f_{cm}$ (MPa) | $E_{cm}$ (MPa) | $f_{ctm}$ (MPa) | $f_y$ (MPa) | $E_s$ (MPa) |
| 8x8_D8 | 39.52 | 32789 | 3.07 | 561.50 | 192800 |
| 9x9_D12 | 40.94 | 31198 | 3.18 | 541.22 | 197770 |
| 10x10_D12 | 37.65 | 34939 | 2.96 | 541.22 | 204953 |
| 10x10_D16 | 39.52 | 32789 | 3.07 | 551.51 | 191250 |
| 12x12_D12 | 39.52 | 32789 | 3.07 | 541.22 | 195864 |

The concrete compressive strength $f_{cm}$ was tested on three 150mm cubes, the modulus of elasticity $E_{cm}$ was tested on three cylinders of size 150mm diameter-300mm height and the tensile strength $f_{ctm}$ was established by means of a tensile splitting strength test on three similarly sized cylinders. Additionally, Table I reports the steel yielding strength $f_y$ and modulus of elasticity $E_s$ established in accordance with ISO 6892-1:2009 (specified in the standard BS EN 10025).

### 2.3 Experimental setup

The members were tested in tension by means of a Universal Testing Machine (UTM). The loading program was a simple displacement-controlled monotonic tensile load increased at a constant speed of 1.0mm/min until the yielding of the rebar is reached. The strains inside the members were monitored through 1.2m long DOF sensors (bonded to the rebars) by means of an OBR ODiSI-A manufactured by LUNA Technologies[33] (Figure 2d). The selected spatial resolutions are 5mm and 7.5mm with measurements every 3 to 5 seconds.

The concrete prisms' surface displacements are, instead, measured through DIC technology. As mentioned earlier, in order to perform a DIC analysis, each image must have a clear pattern that is later divided into a grid of interrogation cells containing a finite number of pixels. Therefore, the resolution and accuracy of the displacement and deformation fields depend on the total number of pixels within the images and on the level of suitability of the pattern to the expected displacements. In order to act on the first point, the utilized camera was a Canon EOS 77D able to take pictures with a resolution of 6000x4000 pixels (24 megapixels) therefore leading to a ratio between 6.6px/mm and 10px/mm according to the orientation of the shots. The camera was positioned 70cm away from the members (Figure 3), perpendicular to the intersection between its vertical and horizontal axis. The stochastic pattern, instead, was sprayed with black matte paint but only after the member's concrete surface was primed with white paint in order to create an even background. Finally, an LVDT was glued to the member's surface in order to ascertain the correctness of the DIC measurements.

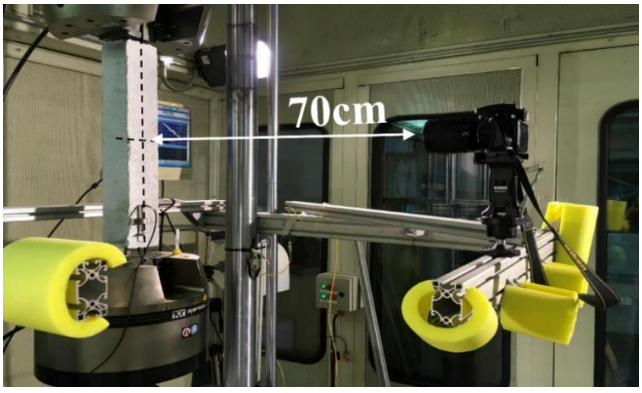


***Figure 3.*** *Tensile test and Digital Image Correlation setup*

## 3. DOFS for the strain monitoring of steel rebars embedded in RC ties: results

As discussed in the previous section, the first step towards a DOFS-powered assessment of a RC structures' bond stresses and slips is the monitoring of their steel rebars' strains and the extraction of their profiles. The present section is, therefore, entirely dedicated to it. With the goal of elucidating the post-processing steps necessary to extract clear and analysis-ready profiles, a modus-operando sub-section is presented, followed by the DOFS strain profiles of cracking and non-cracking members. Finally, in order to set the groundwork for the bond/slip analysis, it is crucial to first elucidate how these two evolve along a RC tie test. Thus, a concise theoretical explanation of the phases that characterize the steel/concrete interaction during such test is inserted parallelly to the results.

### 3.1 Modus operando of a DOFS output post-processing

In the present subsection a detailed example of a DOFS monitored test data post-processing is presented with the intention of elucidating its steps. The study case RC tie is member 8x8_D8. Figure 4 represents its rebar strain evolution along the test as sampled by DOFS.

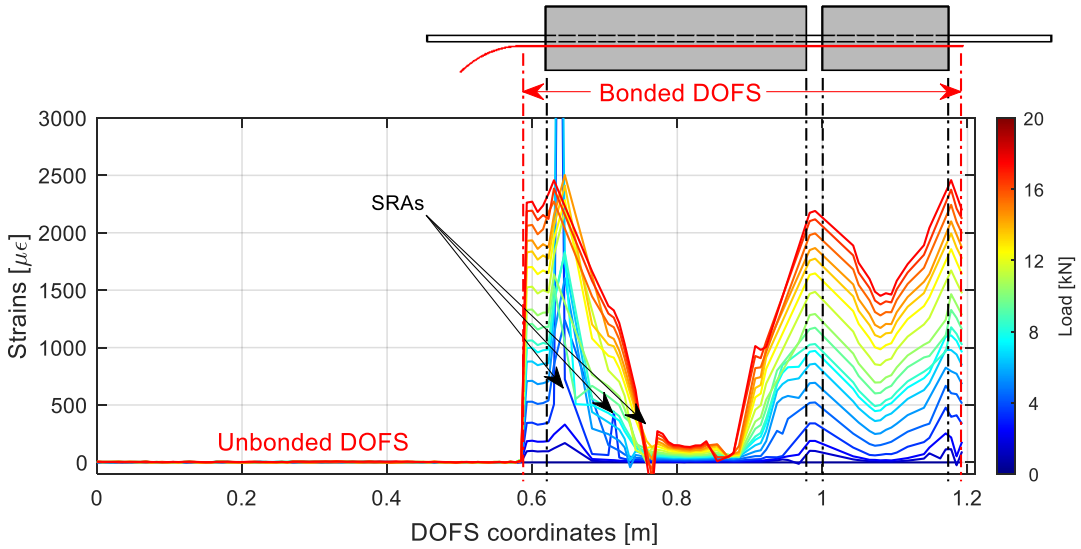


***Figure 4.*** *Member 8x8_D8's DOFS-measured steel strains at various load stages*

In order to help the interpretation of this figure and all the other members' DOFS profiles, Table II clarifies which portion of each DOFS fiber is bonded to which segment of their respective RC ties (this data should be studied in combination with Figure 2a's). Table II displays the first and last DOFS coordinates bonded on the members, suggesting that those in between are the ones effectively monitoring its strains (whether these are pertinent to segments of bare rebar or embedded inside concrete). The strain readings related to DOFS coordinates preceding the first "DOFS monitored section" (usually oscillating around the value of 0με) are irrelevant as they are originated in un-bonded and loose fiber segments (labeled as "unbonded DOFS" in Figure 4). Furthermore, the table elucidates the DOFS coordinates corresponding the start and end of different concrete blocks. When a member includes two blocks, their intermediary DOFS coordinates, being outside of any concrete prism, report the tension-stiffening-deprived bare rebar's strain.

*Table II. Significant DOFS coordinates for the study case RC tensile members*

| Label | First DOFS monitored section (m) | Block 1 | | Block 2 | | Last DOFS monitored section (m) |
|---|---|---|---|---|---|---|
| | | Dimensions (mm) | DOFS coordinates (m) | Dimensions (mm) | DOFS coordinates (m) | |
| 8x8_D8 | 0.5800 | 330 | 0.6300-0.9600 | 160 | 1.0000-1.1600 | 1.19 |
| 9x9_D12 | 0.6900 | 150 | 0.7300-0.8800 | 300 | 0.8900-1.1900 | 1.19 |
| 10x10_D12 | 0.4950 | 600 | 0.5200-1.1200 | - | - | 1.125 |
| 10x10_D16 | 0.5100 | 145 | 0.5550-0.7050 | - | - | - |
| 12x12_D12 | 0.6675 | 190 | 0.7365-0.9365 | 240 | 0.9375-1.1775 | 1.245 |

Returning to the example member 8x8_D8, a correct reading of its DOFS coordinates, as per Table II, should go as follows. The first DOFS coordinate bonded to the rebar and effectively reporting useful strain measurements is 0.58m (as expected, only strain values oscillating around 0με are shown in Figure 4 before such coordinate). The fiber keeps monitoring the bare rebar until DOFS coordinate 0.63m (flat segment in Figure 4) after which it starts reporting the rebar's strains when embedded inside a 330mm long concrete prism. From 0.96m to 1.00m the measurements correspond to the bare rebar situated between the two concrete prisms (again a tiny flat segment can be seen in Figure 4). Between 1.00m and 1.16m the fiber reports the rebar's strains when embedded inside a 160mm long concrete prism. Finally, between 1.16-1.19m the fiber is once again bonded to the bare rebar on the opposite end of the RC tie.

Figure 4's strain data plots are the result of a certain amount of post-processing of their raw counterpart extracted from the OBR. The post-processing is finalized to the removal of as many Strain Reading Anomalies (SRAs) as possible being the latter fictitious and erroneous strain readings caused by failed light backscattering and algorithmic interpretation errors[34]. In order to swiftly elucidate the base mechanism of the adopted post-processing algorithm named Polynomial Interpolation Comparison Method (PICM)[35], it is important to distinguish harmless SRAs (HL-SRAs) from harmful ones (HF-SRAs). The former is a kind of anomaly which, whenever it first occurs in a specific DOFS coordinate, it may still be followed by reliable readings. The latter, instead, it is followed strictly by flawed strain measurements for the remainder of the experimental test. Their elimination procedure differs substantially. Starting from the elimination of HL-SRAs, being this anomaly punctual in nature, the trend of every DOFS coordinate is studied (automatically or otherwise) as in Figure 5a.

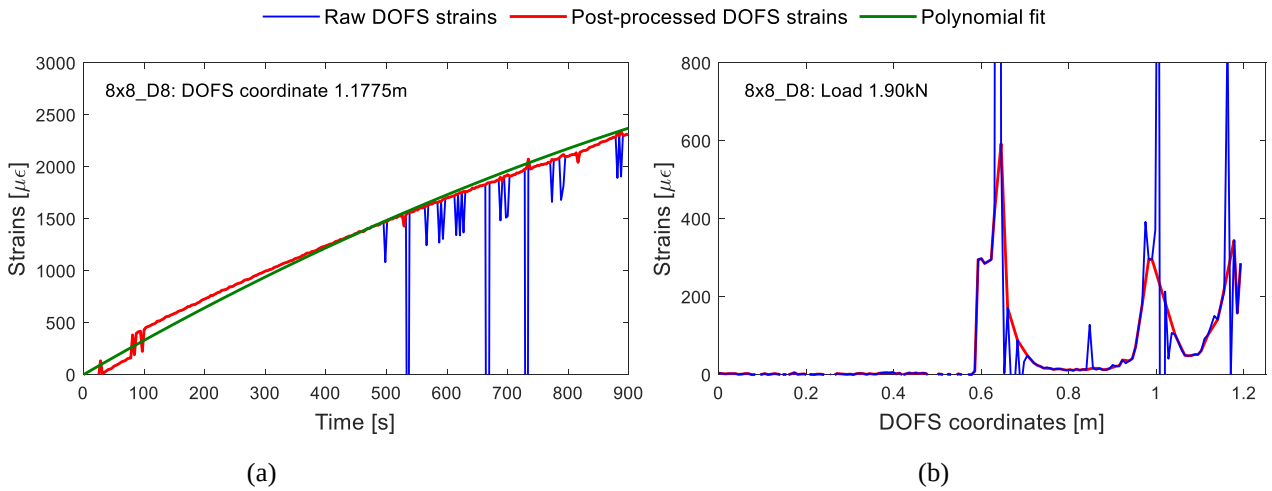


(a) (b)

***Figure 5.*** *DOFS measured steel strains versus time (a) and DOFS coordinates (b)*

The figure displays the strains sampled in a single DOFS coordinate (in blue) and a global trend fit as computed by the PICM algorithm (in green). The latter then investigates the difference between the two profiles. At each x-coordinate, the raw data under consideration is deemed valid (in red) strictly if the difference between the two is less than a defined threshold equivalent to the desired sensitivity of the comparison. For example, the current test used a 150με threshold as it allowed for the removal of the anomalistic peaks whilst leaving untouched any profile jump resulting from real-life occurrences to the tested member (such as concrete cracking). If, instead, the studied raw data is deemed invalid, it is replaced by a linearly interpolated value of the first reliable strain reading measured before and after the faulty data. Moving on to HF-SRAs, these are much harder to diagnose by means of an automated algorithm. Hence, the DOFS coordinates displaying the signs of such anomaly are manually substituted, once again, by means of a linearly interpolated value of the first reliable strain reading measured before and after the specific DOFS coordinate. The results of such post-processing is visible in Figure 5b where the original data (in blue) is overlapped with the processed data (in red).

Despite the DOFS extracted strain profiles having been subjected to the process of SRA-removal, in some occasion the sheer number and size of the anomalies makes it impossible to plot completely SRA-free strain profiles. For example, this is particularly evident in Figure 4's DOFS sections 0.62-0.75m where hardly any data can be considered reliable, especially compared to its much improved symmetrical counterpart (0.85-0.98m). Oppositely the entirety of the second block (0.99-1.15m) presents optimal strain evolution readings.

Only once the SRA-cleansing process is finalized, the strain profiles can finally be considered viable for structural analysis.

### 3.2 DOFS strain monitoring of cracking RC ties

As previously suggested, before presenting any bond stress and slip results, it is crucial to understand how they evolve and change along a RC member test. Therefore, keeping in mind the RC ties' potential of properly depicting the distribution of internal forces and strains inside the RC structures' tensile zones, the present sub-section complements the DOFS steel strain profiles of the tested cracking ties with a short theoretical explanation of their various behavioral phases.

When serviceability is considered, the behavior of a RC member is generally divided in three stages: the *elastic stage*, the *crack formation stage* and the *stabilized cracking stage*. Figure 6 portrays the theoretical profiles of a RC tie's rebar strains $\varepsilon_s(x)$ and steel-concrete bond stresses $\tau(x)$ during these three stages.

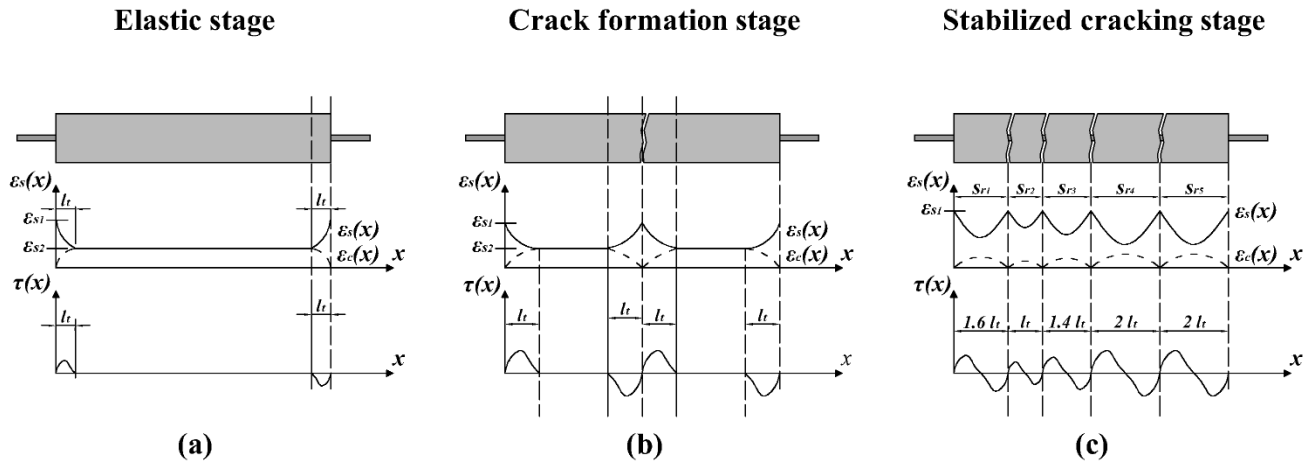


***Figure 6.*** *RC tensile member three stages behavior: elastic (a), crack formation (b) and stabilized cracking (c)*

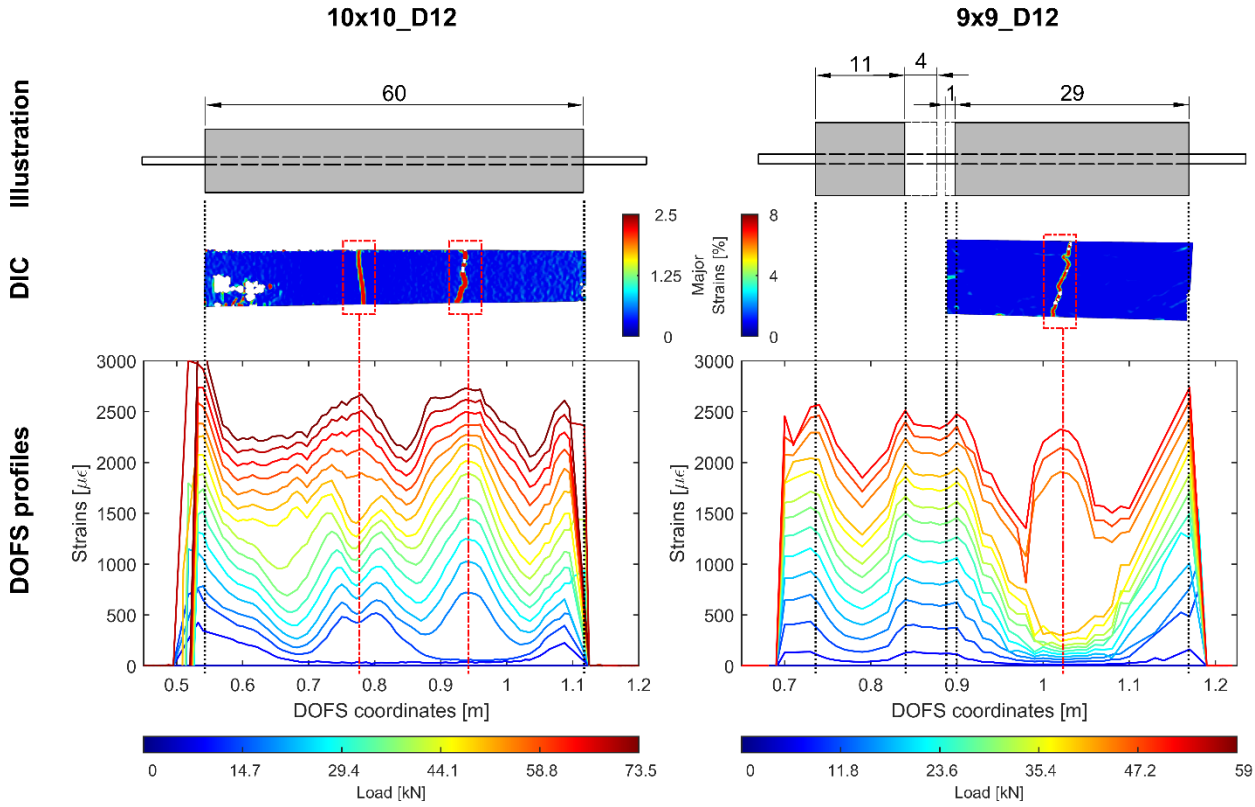


***Figure 7.*** *10x10_D12 (a) and 9x9_D12 (b) correlation between their designed dimensions, DIC analysis and DOFS extracted strain profiles*

Meanwhile, Figure 7 follows up displaying the experimental equivalent of Figure 6's steel strain profiles. In particular, it displays the DOFS-captured profiles of member 10x10_D12 and 9x9_D12 together with their respective substantiating DIC-based major strains analyses. The latter are aligned with their corresponding DOFS coordinates in order to create a tight geometrical correlation between the two experimental outputs.

With these two figures at hand, it is now possible to study in depth the evolution of the DOFS strains along the three above mentioned stages. The first is referred to as elastic stage as no permanent deformations are present, neither in the concrete (cracks) nor in the steel (yielding). At this stage, bond stresses and slip occur strictly within localized regions at the opposite ends of the element. These regions of length $l_t$ (defined as *transmission length*) are where the stresses get transferred from the rebar to the surrounding concrete by the bond stress $\tau$. As a result of this mechanism (defined as *tension-stiffening*) the rebar is increasingly less stressed the deeper it is embedded inside the concrete. This translates in the downwards trending segments visible in the $\varepsilon_s$ profile's extremities in Figure 6a. Beyond the $l_t$, its strains $\varepsilon_{s2}$ (Equation 3) are decidedly inferior compared to the bare rebar's $\varepsilon_{s1}$ (Equation 2).

$$\varepsilon_{s1} = \frac{\sigma_s}{E_s} = \frac{P}{A_s E_s} \tag{2}$$

$$\varepsilon_{s2} = \varepsilon_c = \frac{P}{A_c E_c + E_s A_s} \tag{3}$$

Being $A_s$ the steel rebar's cross-sectional area, $\varepsilon_c$ the concrete's strain and $A_c$ the concrete's cross-sectional area. At the elastic stage, the middle region of the member sees both steel and concrete share the same strain level thus resulting in a flat steel strain profile (*strain compatibility area*) with values equals to $\varepsilon_{s2}$. Experimentally-wise, both the middle and the edges' trends are captured by DOFS as evidenced by Figure 7's lower profiles.

As the applied tensile load increases, eventually the stresses transferred to the concrete surpass its tensile strength $f_{ct}$ leading to the next stage; the crack formation one. Indeed, newly formed peaks are clearly visible in Figure 7 suggesting the appearance of cracks (confirmed by the DIC). Similar profiles are extracted by Michou[36] for an identical cross section/rebar diameter member. In the cracked section the steel rebar cannot transfer anymore the stresses to the concrete (as it is absent) and has to again carry its entirety alone, similarly to what happens on the member's edges. As foreshadowed in Figure 6b, this translates to a peaking of the $\varepsilon_s$ profile in correspondence to the crack. The formation of this strain peak is quite sudden as the bar abruptly passes from carrying a total strain of $\varepsilon_{s2}$ to a much larger one ($\varepsilon_{s1}$) in an instance (a jump of magnitude equivalent to Equation 4).

$$\frac{\varepsilon_{s2}}{\varepsilon_{s1}} = \frac{n * \rho}{1 + n * \rho} \tag{4}$$

In truth, this is often not entirely the case as cracks frequently tend to develop obliquely over multiple cross-sections (as visible in Figure 7's DIC images) due to the heterogeneous distribution of aggregates and lack of tensile strength symmetry across a RC tie's cross-section. Therefore, even in a cracked cross-section, a certain amount of stress is transferred from the bar to the surrounding concrete portions that are still whole thus preventing its strains from reaching the value $\varepsilon_{s1}$, as in Figure 7's DOFS profiles. Furthermore, in the latter, it can be observed that the left crack has a double tip. These eventually merge into one at larger loads probably due to the complete loss of concrete/steel bond between these two tips. Moving away from the crack, concrete is again present around the rebar. Consequently, the steel is able, once more, to transfer to it part of its stresses. This occurs until a point (distant $l_t$ from the crack) beyond which the strain compatibility is fully re-acquired, translating again in a uniformly flat strain profile (as the one visible on the right of 10x10_D12's double-pointed peak). Soon after the advent of the first crack though, crack 2 appears in the middle of the compatibility area and develops much faster than crack 1 due to its superior width.

The third and last stage is the one of stabilized cracking (represented in Figure 6c). Here, despite the increase of the tensile load, the RC tie does not crack any further. This is due to insufficient length of the cracks-defined chunks to allow for the stresses in the concrete to surpass the tensile strength $f_{ct}$. According to the literature[37], the average length of such blocks $s_{rm}$ is considered to be comprised in the interval $l_t<s_{rm}<2l_t$. Experimentally wise, the higher profiles of Figure 7a and b lack any further crack-induced peaks suggesting that the stabilized cracking stage is effectively ongoing. The profiles simply keep increasing in magnitude shifting upwards in the graph. It is also noticeable how, at higher loads, the strain peaks values become similar and equivalent to the bare rebar's due to the full opening of the cracks.

Overall, the above DOFS measurements are in good agreement with the theoretical RC tie behavioral phases. Indeed, the various stages are accurately reported both at low and high strain gradient and absolute value. On the topic of the maximum measurable strain threshold both members continue sampling reliable measurements beyond the cracking stage, deep in the stabilized cracking stage up until the steel yielding strain. This testifies to the resistance of the DOFS as embedded sensors. Finally, a good agreement can also be found between the crack positioning as reported by DOFS and by DIC demonstrating each other's compatibility and integration potential.

### 3.3 DOFS strain monitoring of non-cracking RC ties

The smaller RC ties tested in the present campaign are incorporated in members 8x8_D8, 10x10_D16 and 12x12_D12 (as visible in Figure 2a). Unexpectedly, the former's larger segment (330mm) didn't crack transversally as by design; instead, only splitting cracks appeared on its edges. Indeed, Figure 4 shows no crack-indicative strain peaks effectively suggesting that both segments of 8x8_D8 behave as a non-cracking members. This can be attributed to the lack of sufficient transversal pressure, usually provided by thick concrete covers or transversal reinforcement (both lacking in 8x8_D8), which delays the commencement of splitting failure thanks to its induced frictional force in the steel-concrete contact surface (resulting in higher bond stresses and in reduced values of slip).

Moving on to members 10x10_D16 and 12x12_D12, Figure 8 represents the evolution of their DOFS strain profiles during the tensile test. As visible in Figure 2, on member 10x10_D16 different DOFS/rebar bonding techniques were used.

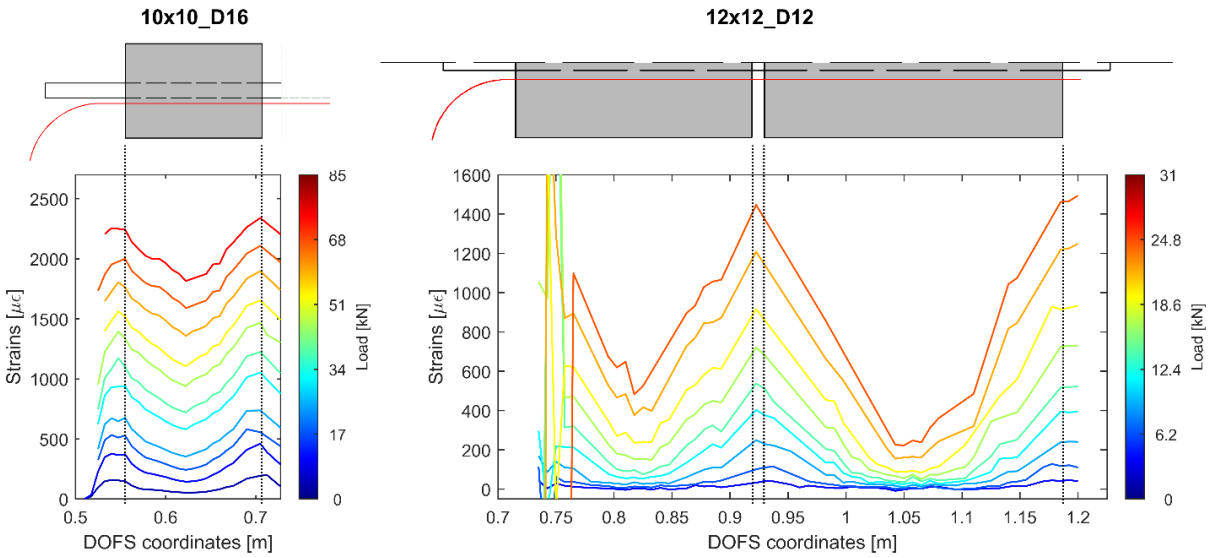


***Figure 8.*** *DOFS Steel strain profiles at various load stages inside member 10x10_D16 (a) and 12x12_D12 (b)*

Its first segment (145mm) is the only one including a silicone-based protection layer and ends up being the only one free of excessive HF-SRAs. Consequently, only the latter is represented in Figure 8a. This result, despite having come at the cost of most of the member's measurements, is crucial for the definition of a universally performant DOFS bonding methodology.

As expected, all of Figure 8's strain profiles present no strain peaks (indicative of cracks) at any load but do, instead, behave in two seemingly different ways. The first, hereon defined as Behavior A and exemplified by member 10x10_D16 (Figure 8a), sees a geometrically uniform evolution of the strain profiles (practically offsetting upwards) proportional to the applied load. Such behavior is also present in the second segment of 8x8_D8 (Figure 4) and in the first segment of 12x12_D12 (Figure 8b). In all of these cases, the strain profiles are initially characterized by a parabolic shape with a flat segment in its center (analogous to the cracking members' elastic stage). Soon after, when the compatibility areas' flatness is lost, they are characterized by two linearly-approximable profiles (crossing in the mid/span) which simply shift upwards remaining almost unaltered. Only the first segment of 12x12_D12, slightly gains pendence with the increasing load. These results are in line with the experimental work from Kankman[7], Beeby and Scott[16], Scott and Gill's[13] and Kaklauskas et al.[1]. Behavior A is reminiscent of the steel rebar's strain profile during the stabilized cracking stage (Figure 6c).

Behavior B, instead, is exemplified by the first segment of 8x8_D8 (Figure 4) and is characterized by a strain profile whose central zone hardly grows along the duration of the test whilst its edges do, proportionally to the load. Such behavior is also evident in the second segment of 12x12_D12 (Figure 8b) even though not as prominently. Behavior B's profiles are reminiscent of Figure 6b's cracking stage ones despite the formers' central zone strains are not sufficiently large for the concrete to actually crack.

The most plausible reason for Behavior A and B's resemblances to the stabilized cracking profiles and cracking stage profiles, respectively, lays in the RC tie lengths. Indeed, member 12x12_D12 second segment's length is critically close to surpassing the member's maximum crack spacing, effectively landing its behavior between a non-cracking and a cracking RC tie. Consequently, its strain profile will be closer to Figure 6b's (cracking stage) than Figure 6c's (stabilized cracking stage) despite never reaching the point that a crack-induced peak appears in its mid-section. Oppositely, member 12x12_D12's first segment, being 50mm shorter, completely misses out on this hybrid behavior therefore being characterized by strain profiles closer to Figure 6c's. In order to assess the correctness of these novel assumptions, further studies should be dedicated to the influence of the tested RC members' longitudinal dimensions on the steel strain profiles.

## 4. DOFS for concrete/steel bond-slip modeling

Similarly to the previous section, this one also presents first a modus operando on how to extract the bond/slip profiles from the DOFS-sampled ones and on how to compare them with the ones calculated according to the Model Code 2010's guidelines. These procedures are then applied to all the RC members. These analyses' outcomes should help gaging DOFS' capacity to lead to accurate bond/slip laws.

### 4.1 Modus operando for DOFS bond-slip calculation

The stress transfer approach considers the strains to be directly governed by the bond-stress between the rebar and concrete on the surface of the former. Yet, the opposite is also valid, therefore the bond-stress $\tau$ can be calculated by simply rearranging Equation 1 into Equation 5.

$$\tau(x) = \frac{E_s \emptyset_s}{4} \frac{d\varepsilon_s(x)}{dx} \tag{5}$$

It should be considered that the DOFS extracted strain profiles aren't fit to be directly used as input for Equation 5's $\varepsilon_s(x)$. Indeed, due to the DOFS' intrinsic sensitive nature, its profiles are never perfectly smooth but rather "lumpy" as visible, for example, in Figure 9a.

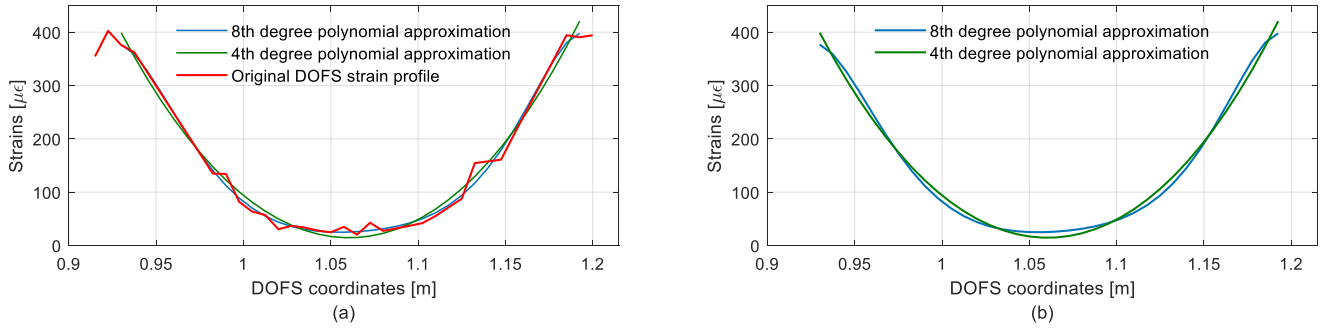


***Figure 9.*** *DOFS extracted strain profile and its different polynomial approximations (a) and just the latter two for better comparison(b)*

The reason for such can span from the DOFS measurement noise to the presence of aggregates in monitored cross-sections creating extra friction on the fiber. However, the overall trend is never less than evident and can be easily captured by means of simple polynomial approximations of any specific degree. For example, Figure 9 represents the use of a $4^{th}$ and $8^{th}$ degree and, as evident in Figure 9b, their resulting profiles display some dissimilarities. In the light of such polynomial-degree profile differences, the choice of the correct degree is crucial for a performant analysis and thus should be undertaken with care.

The steel/concrete slip, over a segment *n* (underscore letter in the following equations) of length $\Delta l$, is calculated as in Equation 6 while the total slip over half of the member *l/2* is a simple integral as in Equation 7.

$$\Delta s_n = \Delta l \left( \frac{\varepsilon_{s,n} + \varepsilon_{s,n-1}}{2} - \frac{\varepsilon_{c,n} + \varepsilon_{c,n-1}}{2} \right) \tag{6}$$

$$\int_0^{l/2} s(x)dx \tag{7}$$

The mean strain in the concrete $\varepsilon_{c,n}$ is calculated by rearranging the equilibrium equation (Equation 8) into Equation 9:

$$P = N_{s,n} + N_{c,n} = \varepsilon_{s,n} E_s A_s + \varepsilon_{c,n} E_c A_c \quad (8)$$

$$\varepsilon_{c,n} = \frac{P - \varepsilon_{s,n} E_s A_s}{E_c A_c} \quad (9)$$

With the bond stress and slip laws defined, they can be compared with the Model Code 2010's ones (Equation 10). The selected parameters to be inserted in Equation 10 are listed in Equation 11 and consider a pull-out failure (double pull-out in our case) and good bonding conditions.

$$\tau_0 = \tau_{max} \left(\frac{s}{s_1}\right)^{\alpha} \; for \; 0 < s < s_1 \quad (10)$$

$$\tau_{max} = 2.5 \sqrt{f_{ck}}\,, \quad s_1 = 1\text{mm} \quad \text{and} \quad \alpha = 0.4 \quad (11)$$

With $f_{ck}$ being the characteristic compressive strength of concrete in our case equals to the members' mean compressive strength $f_{cm}$. By means of these equations, Figure 10 plots the bond stress, slip and bond-slip curves of the study case member 8x8_D8 and, in particular, of the strains included in its DOFS coordinates interval 0.8775-0.9600m. Furthermore, in order to clearly see the profile differences arising when using a specific polynomial degree approximation versus all the others, Figure 10 reports all the curves as calculated by means of 4$^{th}$, 6$^{th}$ and 8$^{th}$ degree polynomial approximations. Their dissimilarity is immediately evident as the ones resulting from higher degree polynomial approximations present more fluctuations as a testament to their increased sensitivity to the strain profiles' own pendence variations. The advantages of higher degree polynomial approximations can be perceived when comparing Figure 10's first and last line. Indeed, in the latter, the graduality with which the steel/concrete strain compatibility is lost along the test is more evident. As a matter of fact, with an 8$^{th}$ degree polynomial approximation, the bond stress graph (Figure 10g) clearly shows how the first DOFS section where $\tau \neq 0$ is progressively shifting inwards with the load, until this condition is only met in the member's mid-span. Differently so, with a 4$^{th}$ degree polynomial approximation, such evolution is undetectable. What is also more discernible in Figure 10g, compared to Figure 10a, is the progressive shift inwards of the bond profiles' maximal points. A correct evaluation of their position is crucial for the definition of the *debonding area* (also defined as bond deterioration zone or damage zone). The latter, comprised between the maximal point on one side and the contiguous member edge on the other, progressively expands inwards as the slip gradually deteriorates the bond. Finally, a higher degree polynomial approximation also represents the rise in the slip (Figure 10b, e and h) in a more realistic fashion.

Oppositely so, the same sensitivity that allows to better represent the bond stress and slip of one RC member, can be counterproductive in another, especially if the latter is "lumpier" than the former. Indeed, with a higher degree polynomial approximation the resulting bond/slip curves of the latter would be characterized by curving and twisting that would not be representative of the global evolution of the bond stress but rather of the influence of punctual factors such as aggregate friction on the fiber and DOFS reading issues. In this case then, a lower degree polynomial approximation is preferable.

The bond/slip curves represented in the upcoming sub-section will follow the above elucidated guidelines.

### 4.2 DOFS bond-slip calculation results

Figure 11 represents the bond stress, slip and their combined law of the other tested members. These plots are obtained by means of polynomial approximations of varying degrees selected on the grounds of the clarity and accuracy of their outputs (as foretold earlier). Furthermore, the MC2010's predicted bond/slip laws have also been included in Figure 11's bond/slip plots for comparison purpose. Note that this comparison's quality index is not a point-by-point similarity between the DOFS and MC2010 curves, but rather a similarity of their magnitude, trend and load-dictated variation.

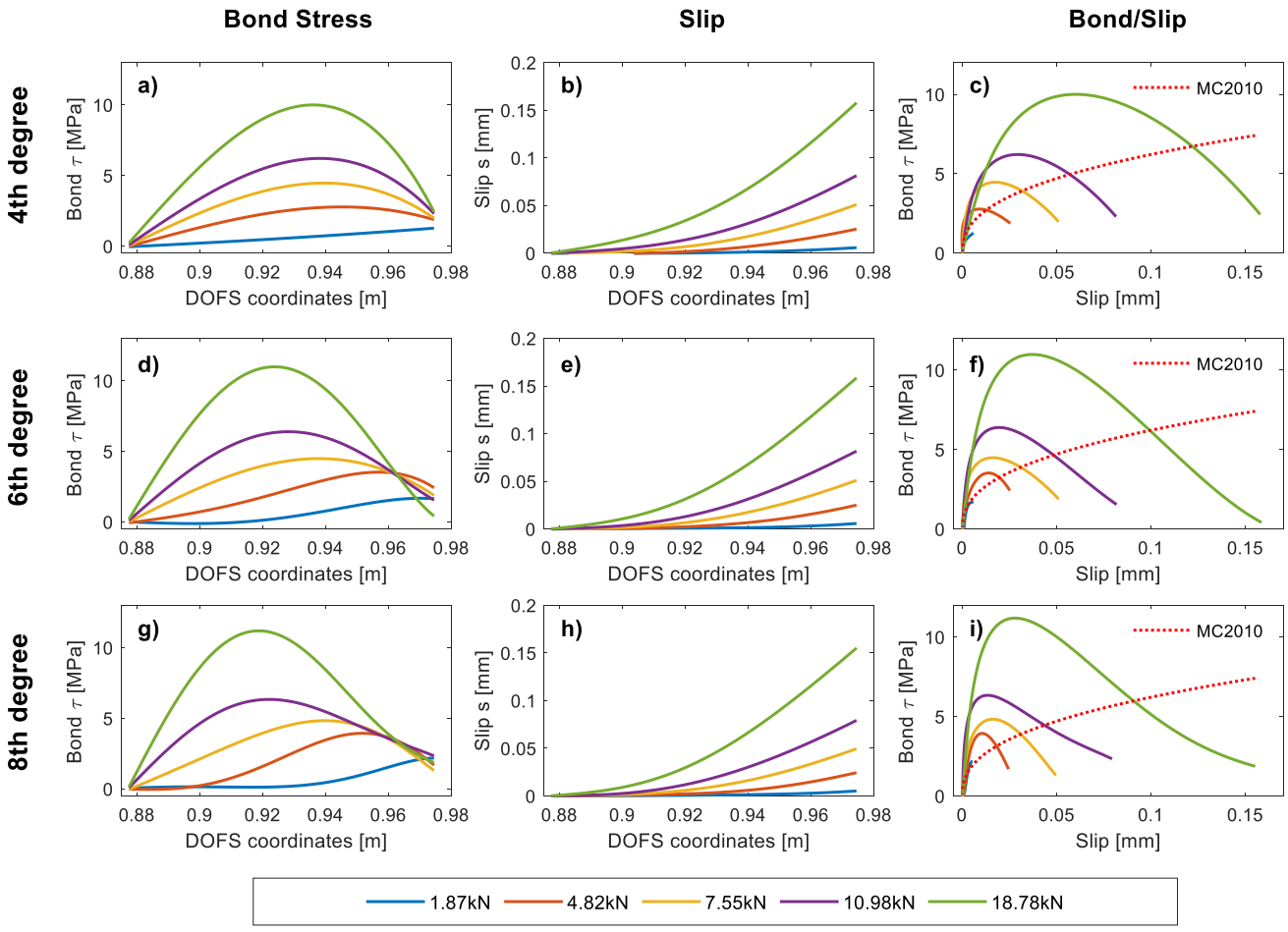


***Figure 10.*** *Bond, slip and bond-slip calculation for 4$^{th}$ ,6$^{th}$ ,8$^{th}$ degree polynomial approximated strain profiles for member 8x8_D8 segment 1*

Also, some of Figure 11's profiles are characterized by smaller final loads compared to the others, namely member 12x12_D12's, due to the disruptive presence of SRAs at larger loads. The use of only low-load profiles is directly reflected in the lower slip values. Finally, for member 9x9_D12, only the first segment's profile (non-cracking) is reported as the precision of the cracking one's is insufficient for a bond/slip analysis.

With these aspects in mind, starting from the concrete/steel bond stress of each member, different development behaviors are noticeable. The first, present in Figure 11a, d, m and p, begins with a few increasingly pendent plots (indicative of the equivalent elastic and cracking phases), but soon after becomes characterized by small variations of mostly linear profiles. Whilst this might not be immediately discernible from Figure 11's bond representations, attention should be put to the load corresponding to each plot. The reader would then see that the ones corresponding to the larger ones are moderately grouped. Differently so, the second development behavior, evident in Figure 10, Figure 11g and j, is characterized by a gradual curvilinear evolution all along the test duration. It should be remarked that member 12x12_D12's segment 1 (Figure 11g) and 10x10_D12 (Figure 11m) display a hybrid behavior, starting with the former and subsequently becoming resemblant to the latter. This, as discussed above, is potentially a consequence of the concrete block's length and its proximity to the minimum crack spacing. The behavioral difference was actually foreshadowed by the dissimilarity of their relative strain profiles and therefore can be tightly correlated to the above defined Behavior A and B.

This difference is also translated in the members' bond-slip laws and is particularly evident when compared against the ones calculated by means of the Model Code 2010. Nowhere is as obvious as in member 8x8_D8's two segments, Figure 10c (or f and i according to the chosen polynomial approximation) and Figure 11c.

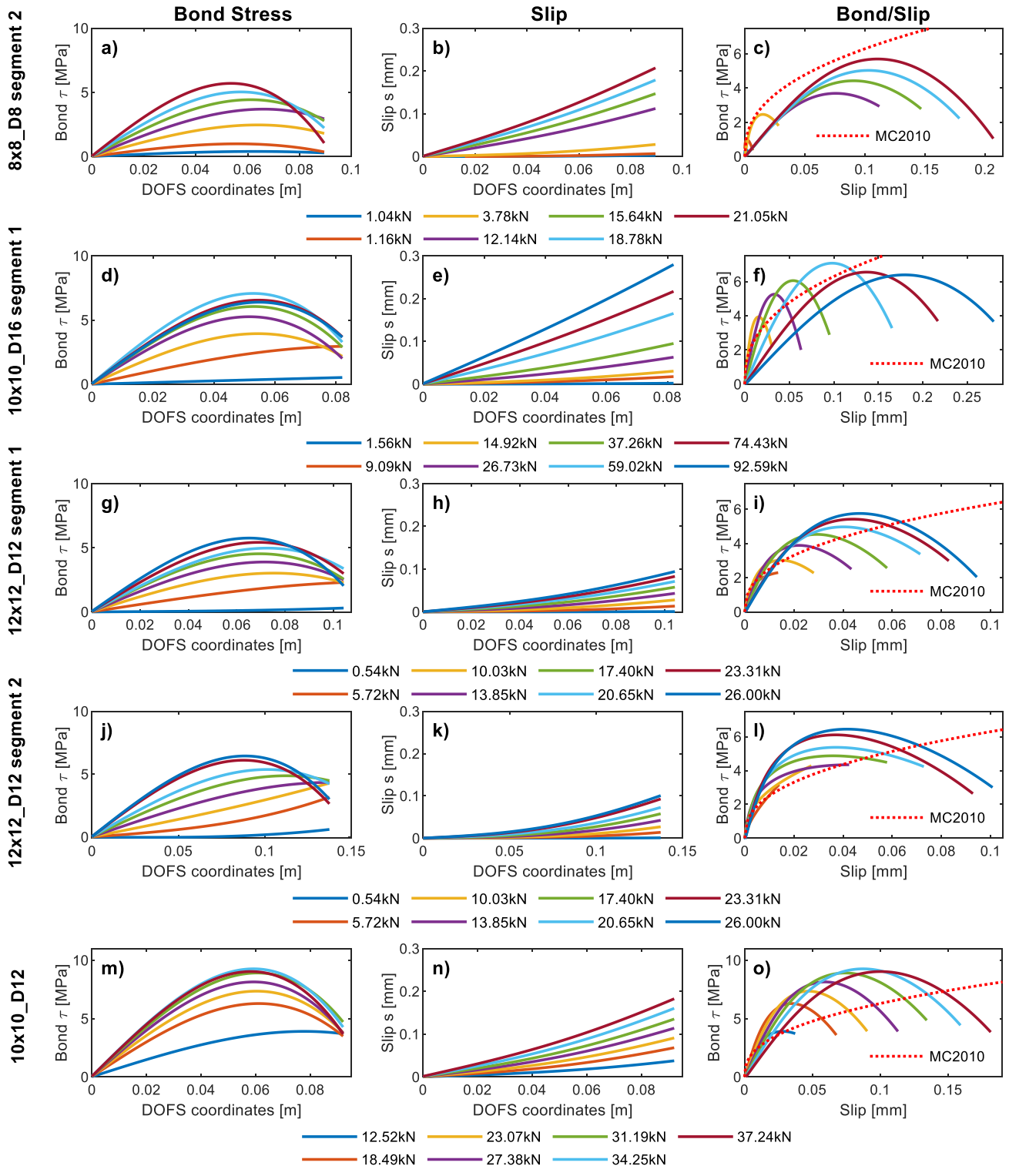
Bond Stress
Slip
Bond/Slip
8x8_D8 segment 2
10x10_D16 segment 1
12x12_D12 segment 1
12x12_D12 segment 2
10x10_D12
a)
b)
c)
d)
e)
f)
g)
h)
i)
j)
k)
l)
m)
n)
o)
Bond τ [MPa]
Slip s [mm]
DOFS coordinates [m]
Slip [mm]
MC2010
1.04kN
3.78kN
15.64kN
21.05kN
1.16kN
12.14kN
18.78kN
1.56kN
14.92kN
37.26kN
74.43kN
9.09kN
26.73kN
59.02kN
92.59kN
0.54kN
10.03kN
17.40kN
23.31kN
5.72kN
13.85kN
20.65kN
26.00kN
12.52kN
23.07kN
31.19kN
37.24kN
18.49kN
27.38kN
34.25kN

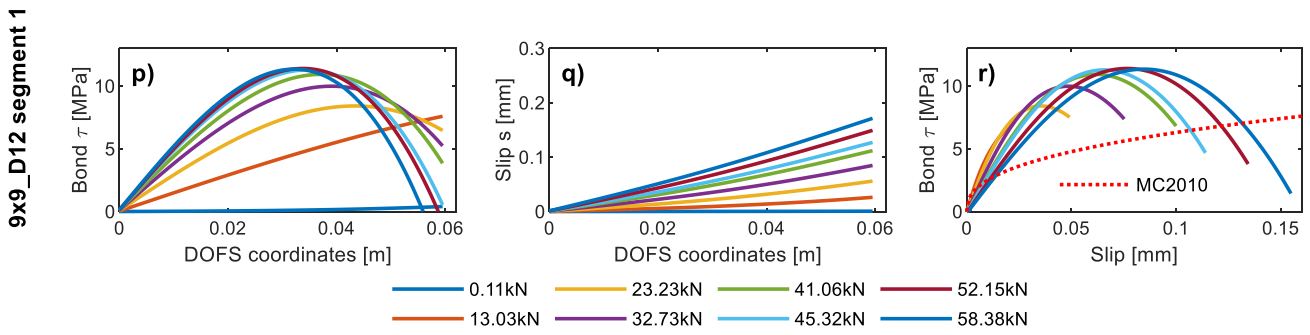


***Figure 11.*** *Bond, slip and bond-slip profiles of members 8x8_D8 segment 2, 10x10_D16 segment 1, 12x12_D12 segment 1 and 2, 10x10_D12 and 9x9_D12 segment 1*

In the former, after a small initial branch of good agreement with the MC2010, the curve's distancing from the code's prediction suggests a much stronger connection between the two constitutive materials compared to the model code's. In the latter, instead, the curve immediately deviates from the model's, thus suggesting a much weaker one. Unfortunately, the order of magnitude of the deviation between the DOFS/MC2010 bond/slip laws cannot be overlooked and seems to advocate for a low reliability of this particular test result (8x8_D8). Then again, this member's compact and almost uniformous bundle of ascending branches can also be found in literature for other bond/slip modeling techniques such as finite elements analysis[38]. Member 10x10_D16's (Figure 11f) ascending branches' pendence coincides with the Model Code's for small loads only. For higher ones, despite still enveloping the MC2010 curve, the profiles fan outwards, losing the compactness that characterized the previous member's profiles. This was to be expected as Behavior A leads by definition to very similar bond stresses but to different slips, thus resulting in ascending branches which tend to distance each other, fanning out, as the load increase. For both 12x12_D12's curves (Figure 11i and l) the resulting bond/slip laws are quite close to the MC2010's predictions; more the former than the latter. The hybrid behavior of Figure 11i's curves is also noticeable as they aren't as compact as in Figure 11j but do not fan out as much as the previous member's. A similar hybrid behavior is noticeable in member 10x10_D12's bond slip laws (Figure 11o) despite its lower proximity to the code's predicted values. This difference persists in Figure 11r in an exacerbated manner.

Figure 12 joins and compares the bond/slip laws (corresponding to Figure 11's largest loads) of both members that include multiple RC blocks (8x8_D8 and 12x12_D12) in order to study the difference among such diversely sized but equally stressed blocks.

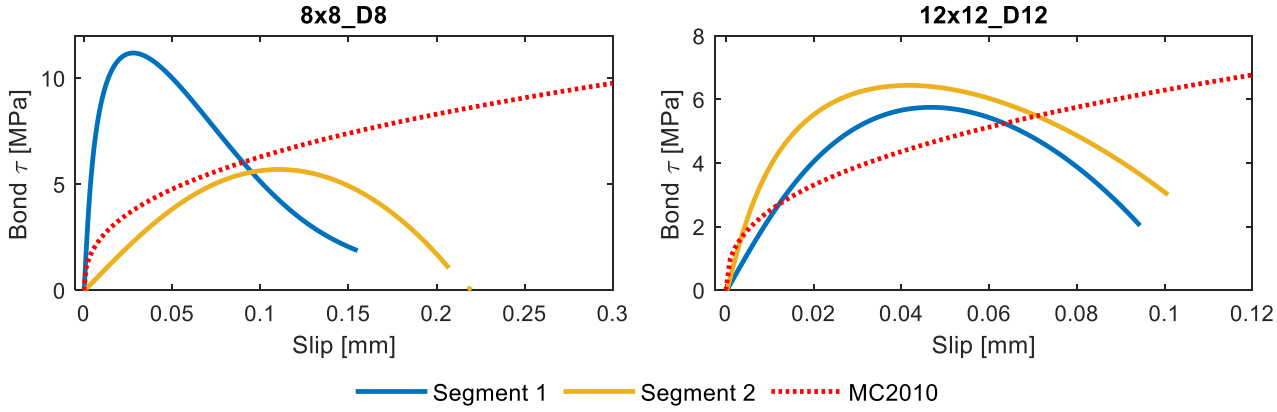


***Figure 12.*** *Bond-slip law comparison with MC2010's for members 8x8_D8 and 12x12_D12*

What is immediately evident is member 8x8_D8's large curves' dissimilarity (absent in 12x12_D12). This suggests a higher quality of the latter's results which, in return, suggests a certain arbitrarity of the result quality extractable by means of a DOFS test. It should be kept in mind that these tests were performed with an ODiSI-A

interrogator model which has seen numerous upgraded versions in the later years, thus this conclusion should be restricted only to such model. Furthermore, the DOFS/rebar bonding technology also covers an influential role on the quality of the results. Indeed, the lack of a protective silicone layer on member 8x8_D8's DOFS (similar to 10x10_D16's first segment's) has proved to be a grave deficiency considering its extensive amount of incurred SRAs. More anomaly-free plot could have potentially yielded improved and more trust-worthy 8x8_D8 bond-slip laws. Moving on to Figure 12's right plot, a much more consistent pair of curves is present which also bring up the interesting interrogative of the influence of the length of the RC blocks on the bond/slip behavior. Indeed, the curves suggest that member 12x12_D12's longer RC block (segment 2) encompasses superior bond stresses for any selected slip value compared to the smaller segment 1. This difference is directly linked to the above mentioned Behaviors A and B which once again is a function of the study case RC block length. Overall, the latter seems to cover an important role in the bond/slip study of RC structure and, as such, it warrants further investigation.

## 4. Conclusions

For a proper study of the serviceability of Reinforced Concrete (RC) structures, the stress transfer approach is considered to be the most suitable methodology as it realistically portrays their inner-workings and, in particular, the interaction between concrete and embedded rebars. Up until the advent of Distributed Optical Fiber Sensors (DOFS), due to the lack of tools able to experimentally assess and accurately quantify such interaction, researchers have resorted to theoretical, empirical or numerical solutions. Thanks to the potential brought forwards by DOFS, this is not required anymore.

DOFS are strain measuring tools whose potential related to the civil engineering field has been discovered only in the latest years. While most applications limit themselves to bonding the DOFS on a structure's surface, a unique utility lies in the possibility of bonding them to the steel reinforcement bars later embedded inside RC structures. This allows for a constant and distributed monitoring of the steel's mechanical strains along their service life or, in our case, along the duration of a laboratory test.

The experimental campaign, topic of the present paper, saw the DOFS strain monitoring of rebars embedded inside multiple cracking and non-cracking RC ties while tested in tension. The goal, to gain insight on the fiber's ability to sample data sufficiently accurate to perform a steel/concrete bond stress and slip assessment analysis. With the help of a Strain Reading Anomalies (SRA)-cleaning post-processing algorithm and polynomial approximations of varying degree to smoothen out the inherently lumpy DOFS strain profiles, the variation of the rebars' strains, the position of the cracks and the members' bond/slip values were extracted. This was achieved for both larger (Ø16) and smaller (Ø8) rebar diameters until the steel yielding stage. Furthermore, the cracking members' cracks position detected by DOFS was compared against the ones detected by a simultaneous Digital Image Correlation (DIC) monitoring. Good agreement between the two was observed, demonstrating the viability of the DOFS/DIC combination for the testing of RC structures.

The DOFS extracted strain profiles and bond/slip laws suggested the presence of a dual behavior of the RC blocks, namely non-cracking RC ties or by RC blocks between two cracks, potentially dictated by their longitudinal size. Indeed, a hybrid behavior between crack formation stage's (named Behavior A) and stabilized cracking stage's (named Behavior B) was found for members whose length is dangerously close to surpassing the maximum crack spacing length but not close enough to allow for the formation of a new crack. This is translated in different bond-slip profiles too. Behavior A's ascending branches tend to fan outwards whilst B's are characterized by a compact ascending trend. Behavioral differences aside, if to compare the DOFS extracted bond/slip graphs with the Model Code 2010's predictions, it can be noticed how DOFS' bonds are consistently larger than the MC2010's per similar slip values. Further research is required to assess whether this discrepancy is substantiated or simply the fruit of an un-performant ODiSI-A's powered DOFS monitoring. Furthermore, for future DOFS applications a combination of gluing adhesive (cyanoacrylate for example) with the addition of a protective layer (silicone) is the preferable DOFS/rebar bonding technique as it removes undesired SRA-related uncertainties.

In conclusion, while DOFS fibers bonded to the reinforcing steel seems to be optimal for crack detection and the derivation of the experimental rebars' strain profiles, further research needs to be developed on the bond-slip prediction potential.

**Acknowledgment:**

The study was performed within project No 09.3.3-LMT-K-712-01-0145 that has received funding from European Social Fund under grant agreement with the Research Council of Lithuania (LMTLT). Furthermore, the authors acknowledge the help of COTCA Asistencia Técnica, Patología y Control de Calidad for the contribution provided in lending the OBR ODiSI-A machine.

**References:**

1. Kaklauskas, G., Sokolov, A., Ramanauskas, R. & Jakubovskis, R. Reinforcement Strains in Reinforced Concrete Tensile Members Recorded by Strain Gauges and FBG Sensors : Experimental and Numerical Analysis. *Sensors* 1–13 (2019). doi:10.3390/s19010200
2. Kaklauskas, G., Gribniak, V., Jakubovskis, R. & Gudonis, E. Serviceability analysis of flexural reinforced concrete members. *J. Civ. Eng. Manag.* **18**, 24–29 (2012).
3. Ruiz, M. F., Muttoni, A. & Gambarova, P. G. Analytical modeling of the pre – and post – yield behavior of bond in reinforced concrete. *J. Struct. Eng.* **133**, 1–27 (2007).
4. Davis, M. B., Hoult, N. A., Bajaj, S. & Bentz, E. C. Distributed Sensing for Shrinkage and Tension-Stiffening Measurement. *ACI Struct. J.* **114**, (2017).
5. Diab, A. M., Elyamany, H. E., Hussein, M. A. & Al Ashy, H. M. Bond behavior and assessment of design ultimate bond stress of normal and high strength concrete. *Alexandria Eng. J.* **53**, 355–371 (2014).
6. Wu, Y.-F. & Zhao, X.-M. Unified bond stress–slip model for reinforced concrete. *J. Struct. Eng.* **139**, 1951–1962 (2012).
7. Kankam, C. K. Relationship of Bond Stress, Steel Stress, and Slip in Reinforced Concrete. *J. Struct. Eng.* **123**, 79–85 (1997).
8. American Concrete Institute (ACI). Building code requirements for reinforced concrete. in *ACI Committee 318* (1995).
9. Beverly, P. *fib Model Code for Concrete Structures 2010*. (2013).
10. Lagier, F., Massicotte, B. & Charron, J. P. Experimental investigation of bond stress distribution and bond strength in unconfined UHPFRC lap splices under direct tension. *Cem. Concr. Compos.* **74**, 26–38 (2016).
11. Ruiz, M. F., Muttoni, A. & Gambarova, P. G. Analytical modeling of the pre- and postyield behavior of bond in reinforced concrete. *J. Struct. Eng.* **133**, 1364–1372 (2007).
12. Houde, J. Study of Force-Displacement Relationships for the Finite-Element Analysis of Reinforced Concrete. (McGill University, Montreal, Quebec, Canada, 1974).
13. Scott, R. H. & Gill, P. A. T. Short-term distributions of strain and bond stress along tension reinforcement. *Struct. Eng. 65B* **65**, 39-43,48 (1987).
14. Murray, A., Gilbert, R. I. & Castel, A. A new Approach to modeling tension stiffening in reinforced concrete. *ACI Struct. J.* **115**, 127–137 (2018).
15. Kaklauskas, G. Crack Model for RC Members Based on Compatibility of Stress-Transfer and Mean-Strain Approaches. *J. Struct. Eng.* **143**, 1–12 (2017).
16. Beeby, A. W. & H. Scott, R. Cracking and deformation of axially reinforced members subjected to pure tension. *Mag. Concr. Res.* **57**, (2005).
17. Ferdinand, P. The Evolution of Optical Fiber Sensors Technologies During the 35 Last Years and Their Applications in Structure Health Monitoring. in *EWSHM-7th European Workshop on Structural Health Monitoring* (2014).
18. LUNA. LUNA ODiSI A ( Optical Distributed Sensor Interrogator ) data sheet.
19. Rodriguez, G. *et al.* Assessing Cracking Characteristics of Concrete Structures by Distributed Optical Fiber and Non-Linear Finite Element Modelling. in *EWSHM-7th European Workshop on Structural Health Monitoring* (2014).
20. Davis, M., Hoult, N. A. & Scott, A. Distributed strain sensing to determine the impact of corrosion on bond performance in reinforced concrete. *Constr. Build. Mater.* **114**, 481–491 (2016).
21. Davis, M. B., Hoult, N. A., Bajaj, S. & Bentz, E. C. Distributed Sensing for Shrinkage and Tension Stiffening Measurement. *ACI Struct. J.* **114**, (2017).

22. Sieńko, R., Zych, M., Bednarski, Ł. & Howiacki, T. Strain and crack analysis within concrete members using distributed fibre optic sensors. *Struct. Heal. Monit.* (2018). doi:10.1177/1475921718804466
23. Quiertant, M. *et al.* Deformation Monitoring of Reinforcement Bars with a Distributed Fiber Optic Sensor for the SHM of Reinforced Concrete Structures. *NDE 2012* 1063–1073 (2012).
24. Brault, A. & Hoult, N. Distributed Reinforcement Strains: Measurement and Application. *ACI Struct. J.* **116**, 115–127 (2019).
25. Poldon, J. J., Hoult, N. A. & Bentz, E. C. Distributed Sensing in Large Reinforced Concrete Shear Test. (2019). doi:10.14359/51716765
26. Broth, Z. & Hoult, N. A. Dynamic distributed strain sensing to assess reinforced concrete behaviour. *Eng. Struct.* **204**, 110036 (2020).
27. McCormick, N. & Lord, J. Digital image correlation. *Mater. Today* **13**, 52–54 (2010).
28. Antoš, J., Nežerka, V. & Somr, M. Assessment of 2D-DIC Stochastic Patterns. in *Acta Polytechnica CTU* 1–10 (2017). doi:10.14311/APP.2017.13.0001
29. Villalba, S. & Casas, J. R. Application of optical fiber distributed sensing to health monitoring of concrete structures. *Mech. Syst. Signal Process.* **39**, 441–451 (2013).
30. Barrias, A., Casas, J. R. & Villalba, S. Application study of embedded Rayleigh based Distributed Optical Fiber Sensors in concrete beams. *Procedia Eng.* **199**, 2014–2019 (2017).
31. Davis, M., Hoult, N. A. & Scott, A. Distributed strain sensing to assess corroded RC beams. *Eng. Struct.* **140**, 473–482 (2017).
32. Brault, A., Nurmi, S. & Hoult, N. A. Distributed Deflection Measurement of Reinforced Concrete Elements Using Fibre Optic Sensors. in *Proceedings of the International Association for Bridge and Structural Engineering (IABSE) Symposium* 1469–1477 (2017).
33. LUNA. ODiSI-A Distributed, Optical Interrogator, Sensor Guide, Users.
34. Bado, M. F., Casas, J. R. & Barrias, A. Performance of Rayleigh-Based Distributed Optical Fiber Sensors Bonded to Reinforcing Bars in Bending. *Sensors* 23 (2018). doi:10.3390/s18093125
35. Bado, M. F., Casas, J. R. & Gomez, J. Post-processing algorithms for distributed optical fiber sensing in structural health monitoring applications. *Struct. Heal. Monit.* (2020). doi:10.1177/1475921720921559
36. Michou, A. *et al.* Reinforcement-concrete bond behavior: Experimentation in drying conditions and meso-scale modeling. *Eng. Struct.* **101**, 570–582 (2015).
37. Kaklauskas, G., Ramanauskas, R. & Jakubovskis, R. Mean crack spacing modelling for RC tension elements. *Eng. Struct.* **150**, 843–851 (2017).
38. Jakubovskis, R. & Kaklauskas, G. Bond-stress and bar-strain profiles in RC tension members modelled via finite elements. *Eng. Struct.* **194**, 138–146 (2019).


(a) (b)

637 ***Figure 1.*** *Distributed Optical Fiber Sensor with loose termination (b) and bonded to a rebar*

638

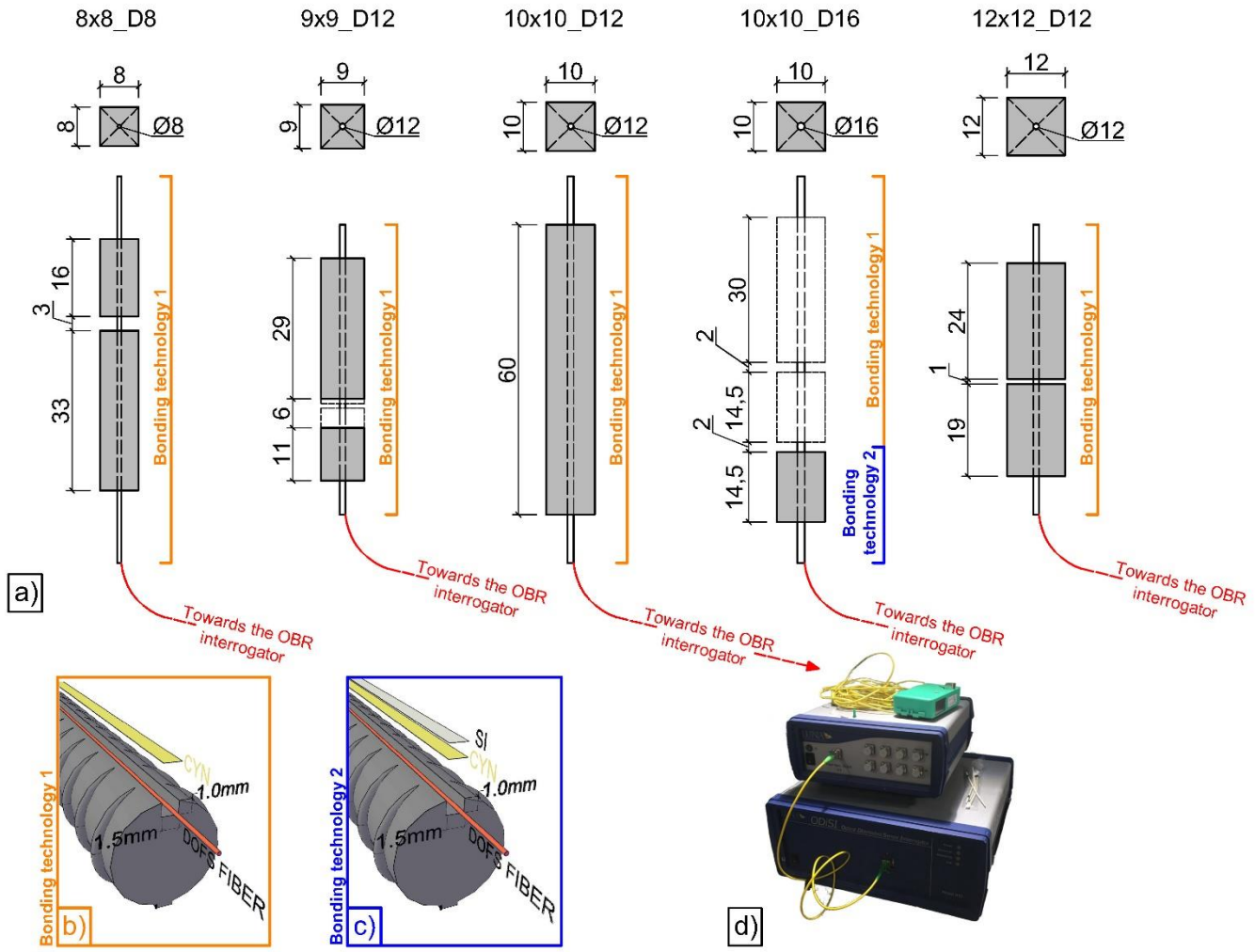


**Figure 2.** *Tested RC ties' geometrical features (a) with their respective bonding technologies with (c) and without (b) the addition of a protective silicone layer. The DOFS-instrumented rebars were monitored by means of an ODiSI-A OBR interrogator (d).*

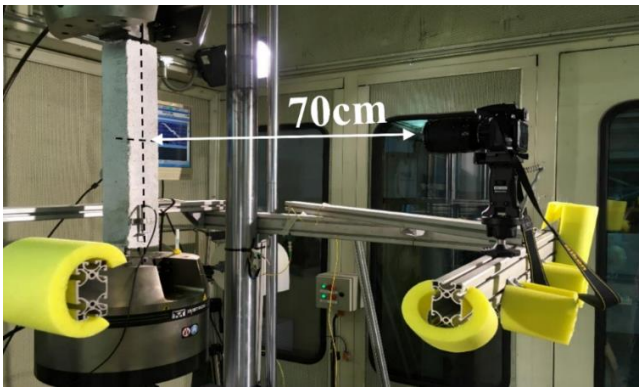


644

645 ***Figure 3.*** *Tensile test and Digital Image Correlation setup*

646

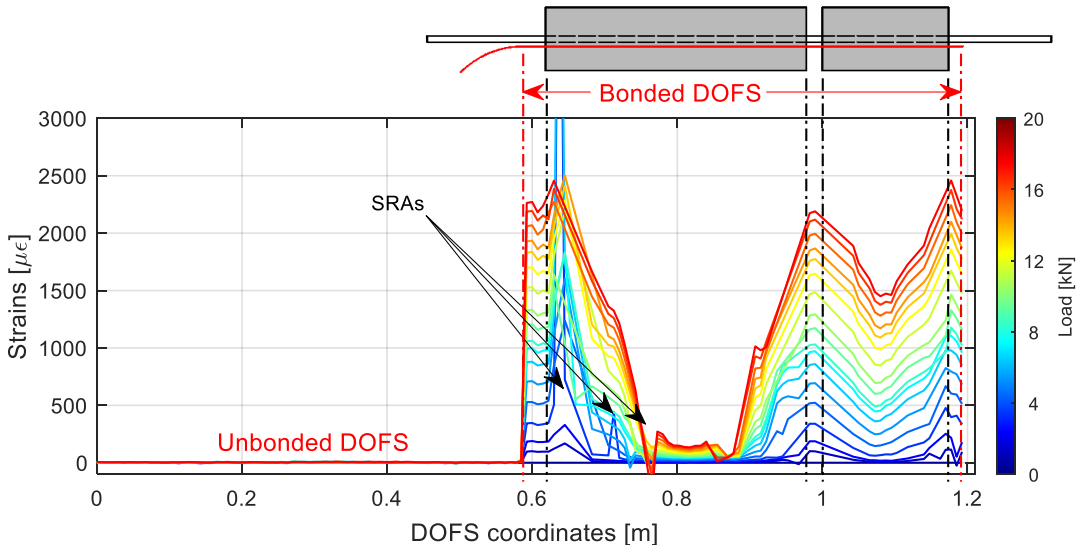


***Figure 4.*** *Member 8x8_D8's DOFS-measured steel strains at various load stages*

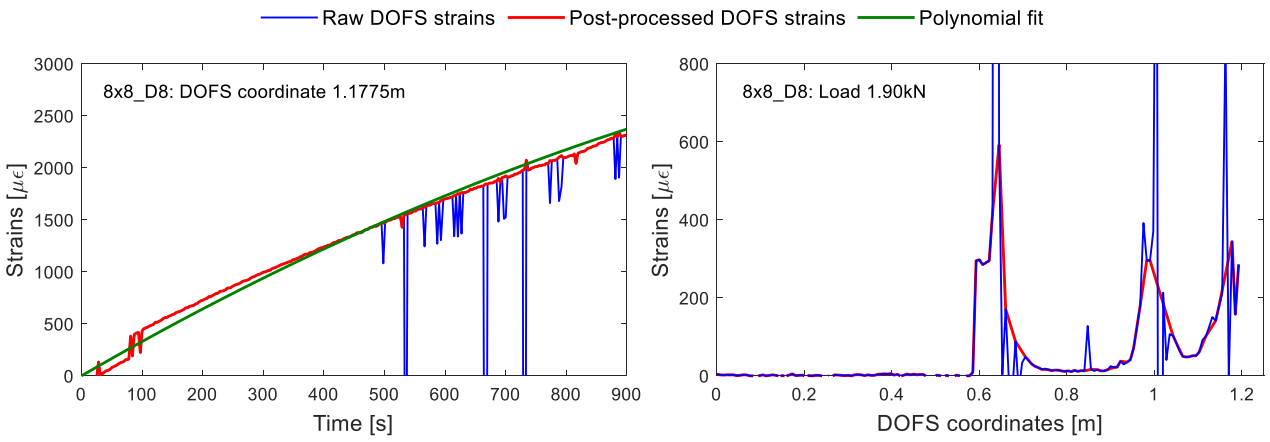


(a) (b)

650 ***Figure 5.*** *DOFS measured steel strains versus time (a) and DOFS coordinates (b)*

651

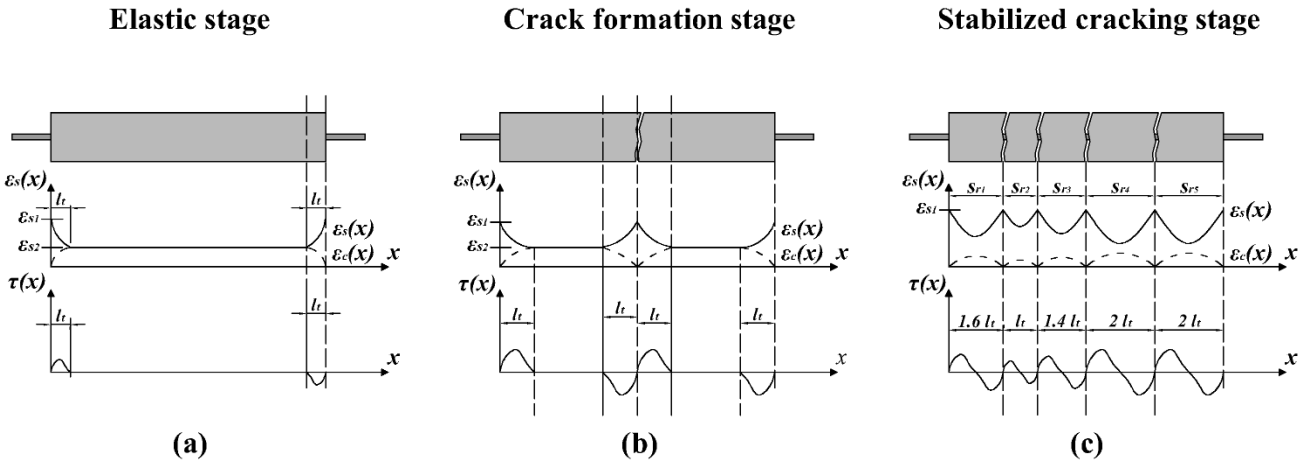


***Figure 6.*** *RC tensile member three stages behavior: elastic (a), crack formation (b) and stabilized cracking (c)*

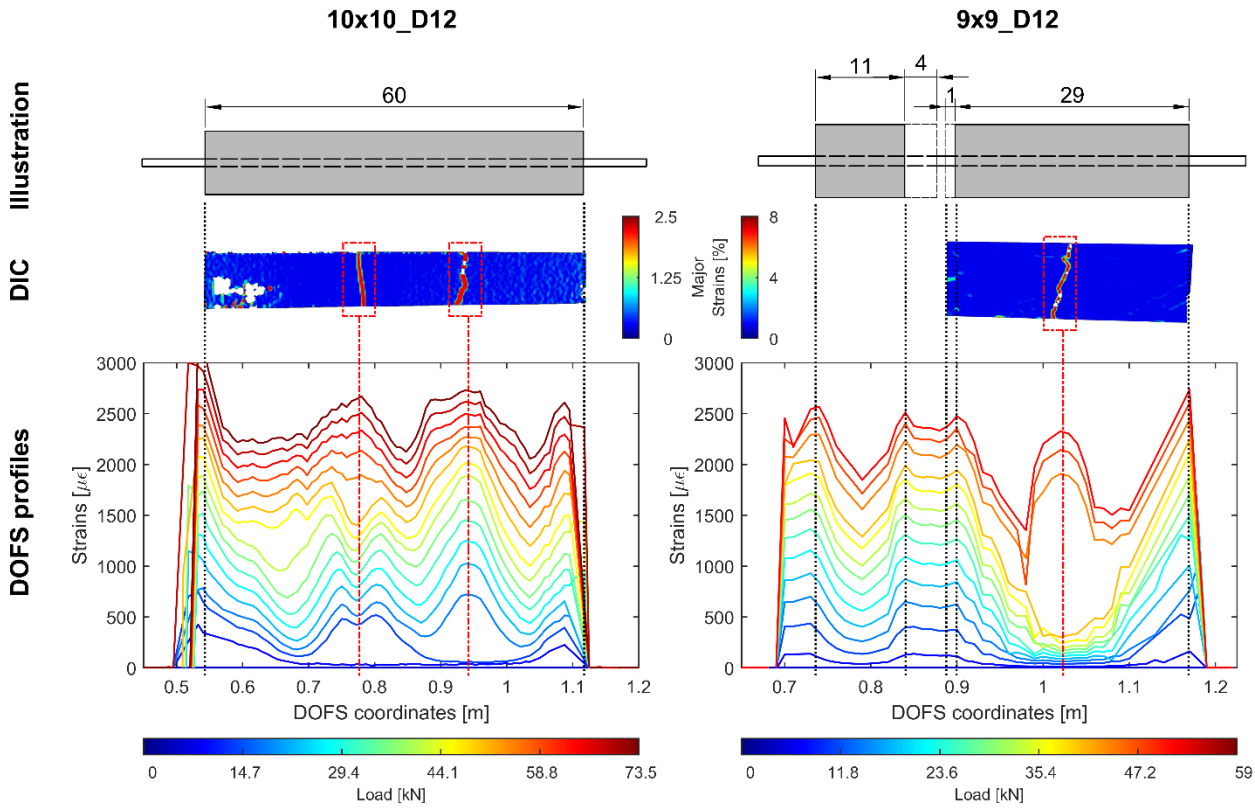


655 ***Figure 7.*** *10x10_D12 (a) and 9x9_D12 (b) correlation between their designed dimensions, DIC analysis and*
656 *DOFS extracted strain profiles*

657

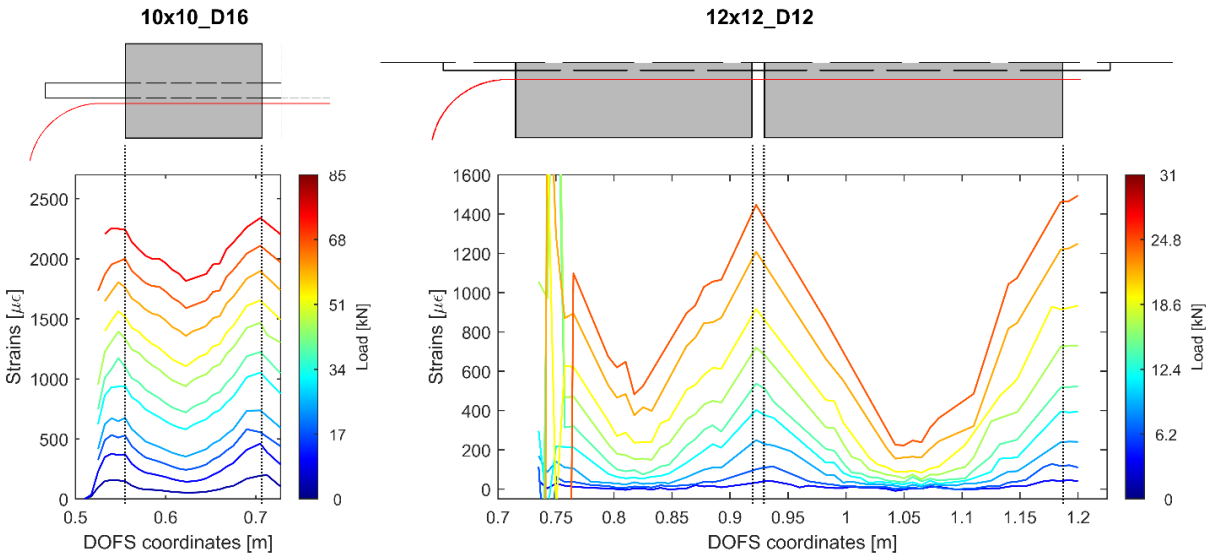


658 ***Figure 8.*** *DOFS Steel strain profiles at various load stages inside member 10x10_D16 (a) and 12x12_D12 (b)*

659

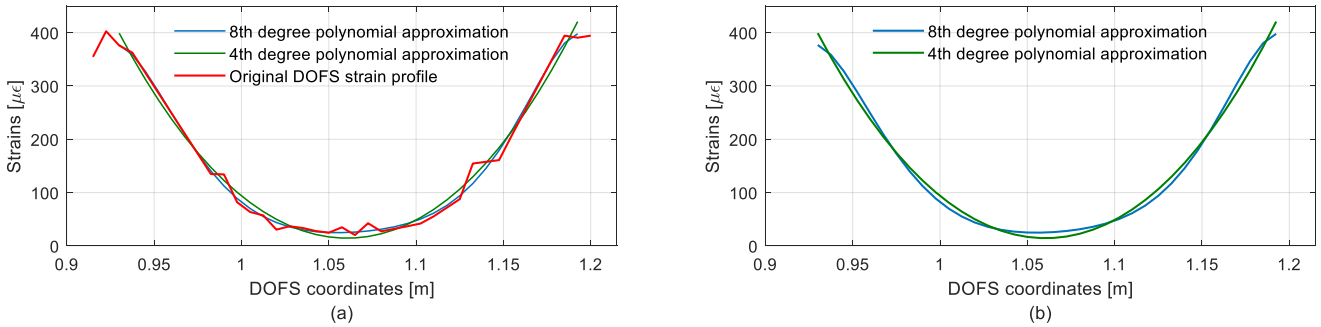


***Figure 9.*** *DOFS extracted strain profile and its different polynomial approximations (a) and just the latter two for better comparison(b)*

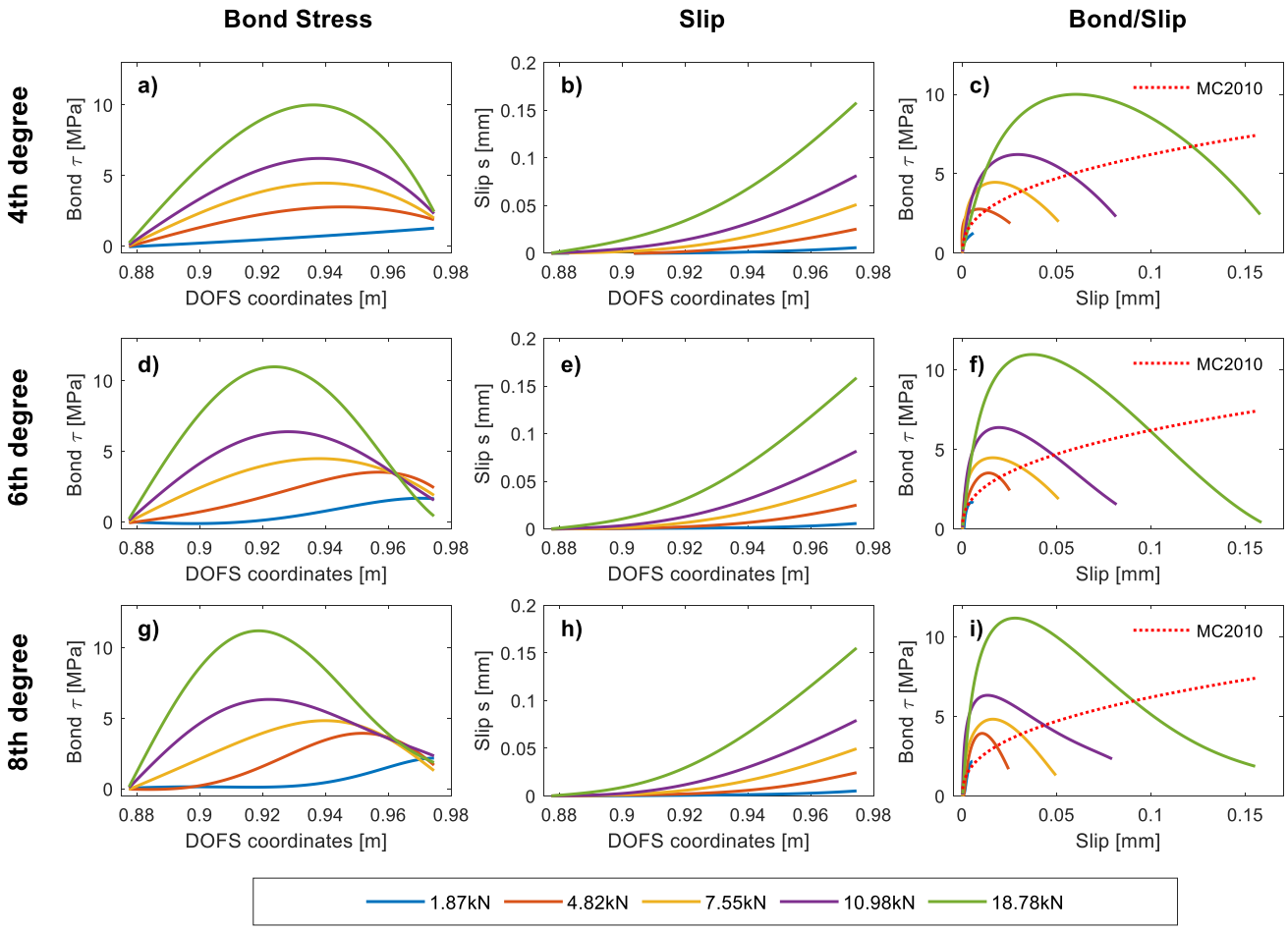


664

665 ***Figure 10.*** *Bond, slip and bond-slip calculation for $4^{th}$ ,$6^{th}$ ,$8^{th}$ degree polynomial approximated strain profiles for*
666 *member 8x8_D8 segment 1*

667

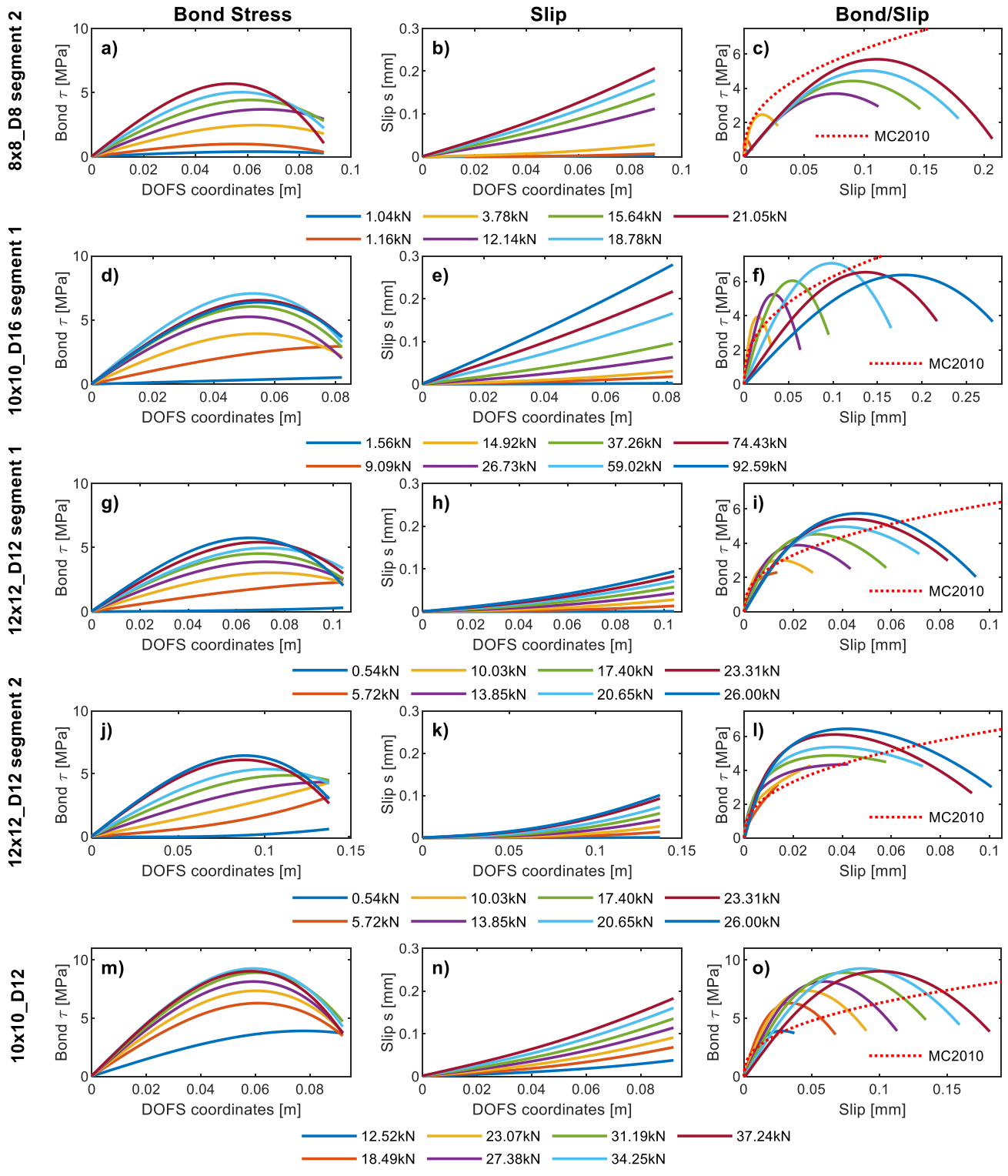
Bond Stress
Slip
Bond/Slip
8x8_D8 segment 2
10x10_D16 segment 1
12x12_D12 segment 1
12x12_D12 segment 2
10x10_D12
a)
b)
c)
d)
e)
f)
g)
h)
i)
j)
k)
l)
m)
n)
o)
Bond τ [MPa]
Slip s [mm]
DOFS coordinates [m]
Slip [mm]
MC2010
1.04kN
3.78kN
15.64kN
21.05kN
1.16kN
12.14kN
18.78kN
1.56kN
14.92kN
37.26kN
74.43kN
9.09kN
26.73kN
59.02kN
92.59kN
0.54kN
10.03kN
17.40kN
23.31kN
5.72kN
13.85kN
20.65kN
26.00kN
12.52kN
23.07kN
31.19kN
37.24kN
18.49kN
27.38kN
34.25kN

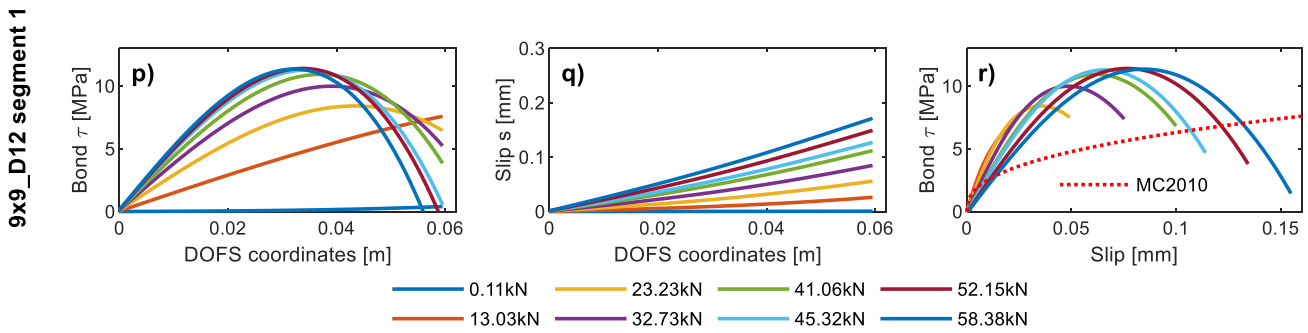


670

671 ***Figure 11.*** *Bond, slip and bond-slip profiles of members 8x8_D8 segment 2, 10x10_D16 segment 1, 12x12_D12*
672 *segment 1 and 2, 10x10_D12 and 9x9_D12 segment 1*

673

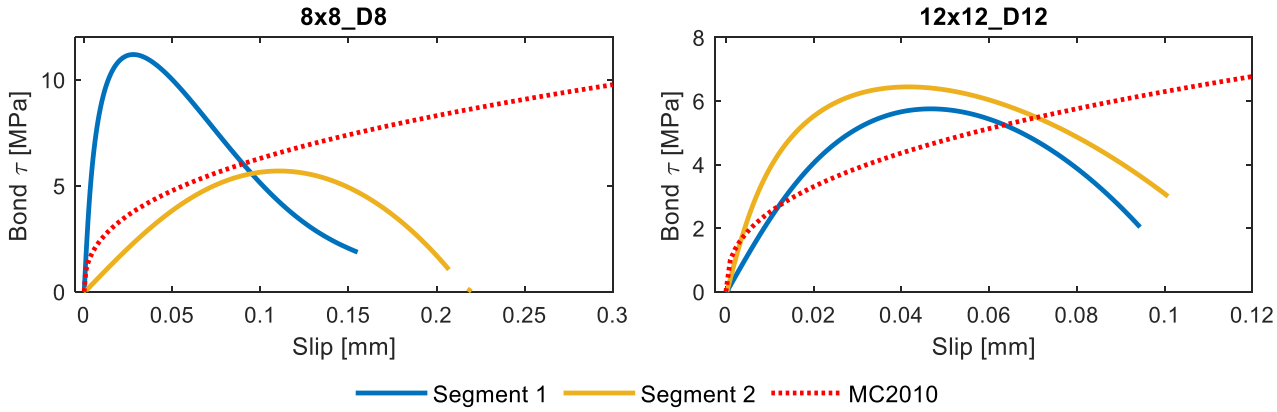


674

675 ***Figure 12.*** *Bond-slip law comparison with MC2010's for members 8x8_D8 and 12x12_D12*

676

**Declaration of interests**

☒ The authors declare that they have no known competing financial interests or personal relationships that could have appeared to influence the work reported in this paper.

☐The authors declare the following financial interests/personal relationships which may be considered as potential competing interests:

Before the advent of Distributed Optical Fiber Sensors (DOFS), due to the lack of tools able to study the steel rebars' strains when embedded inside Reinforced Concrete (RC) structures in an accurate, completely-distributed and un-intrusive fashion, structural analyses that rely on such information (such as tension stiffening) have always resorted to theoretical, empirical or numerical solutions. Yet, with the potential provided by DOFS, such insight is finally acquirable.

The goal of the present paper is to take full advantage of such potential to study the bond stress and slip present on the surface between concrete and steel rebars in differently sized cracking and non-cracking RC tensile members.

The authors believe the work could represent the start of a new way of understanding the composite behavior of RC structures and more in particular the beginning of a novel DOFS-aided bond/slip quantification trend.